Inter-annual trends of ultrafine particles in urban Europe

Meritxell Garcia-Marlès, Rosa Lara, Cristina Reche, Noemí Pérez, Aurelio Tobías, Marjan Savadkoohi, David Beddows, Imre Salma, Máté Vörösmarty, Tamás Weidinger, et al.

Environment International 185 (2024) 108510

Contents lists available at ScienceDirect

Environment International

journal homepage: www.elsevier.com/locate/envint

Full length article

Inter-annual trends of ultrafine particles in urban Europe

Meritxell Garcia-Marlès [a,b,*], Rosa Lara [a], Cristina Reche [a], Noemí Pérez [a], Aurelio Tobías [a], Marjan Savadkoohi [a,c], David Beddows [d], Imre Salma [e], Máté Vörösmarty [f], Tamás Weidinger [g], Christoph Hueglin [h], Nikos Mihalopoulos [i,j], Georgios Grivas [j], Panayiotis Kalkavouras [j,k], Jakub Ondráček [l], Naděžda Zíková [l], Jarkko V. Niemi [m], Hanna E. Manninen [m], David C. Green [n,o], Anja H. Tremper [n], Michael Norman [p], Stergios Vratolis [q], Konstantinos Eleftheriadis [q], Francisco J. Gómez-Moreno [r], Elisabeth Alonso-Blanco [r], Alfred Wiedensohler [s], Kay Weinhold [s], Maik Merkel [s], Susanne Bastian [t], Barbara Hoffmann [u], Hicran Altug [u], Jean-Eudes Petit [v], Olivier Favez [w], Sebastiao Martins Dos Santos [x], Jean-Philippe Putaud [x], Adelaide Dinoi [y], Daniele Contini [y], Hilkka Timonen [z], Janne Lampilahti [aa], Tuukka Petäjä [aa], Marco Pandolfi [a], Philip K. Hopke [bb], Roy M. Harrison [d,cc], Andrés Alastuey [a], Xavier Querol [a,*]

[a] *Institute of Environmental Assessment and Water Research (IDAEA-CSIC), 08034 Barcelona, Spain*
[b] *Department of Applied Physics-Meteorology, University of Barcelona, Barcelona, 08028, Spain*
[c] *Department of Mining, Industrial and ICT Engineering (EMIT), Manresa School of Engineering (EPSEM), Universitat Politècnica de Catalunya (UPC), Manresa 08242, Spain*
[d] *Division of Environmental Health and Risk Management, School of Geography, Earth and Environmental Sciences, University of Birmingham, Edgbaston, Birmingham B15 2TT, United Kingdom*
[e] *Institute of Chemistry, Eötvös Loránd University, Budapest, Hungary*
[f] *Hevesy György Ph.D. School of Chemistry, Eötvös Loránd University, Budapest, Hungary*
[g] *Department of Meteorology, Eötvös Loránd University, Budapest, Hungary*
[h] *Laboratory for Air Pollution and Environmental Technology, Swiss Federal Laboratories for Materials Science and Technology (Empa), 8600 Duebendorf, Switzerland*
[i] *Environmental Chemical Processes Laboratory, Department of Chemistry, University of Crete, 71003 Heraklion, Greece*
[j] *Institute for Environmental Research & Sustainable Development, National Observatory of Athens, 11810 Athens, Greece*
[k] *Department of Environment, University of the Aegean, 81100 Mytilene, Greece*
[l] *Laboratory of Aerosols Chemistry and Physics, Institute of Chemical Process Fundamentals, v.v.i, Academy of Sciences of the Czech Republic, Rozvojova 1, Prague, Czech Republic*
[m] *Helsinki Region Environmental Services Authority (HSY), 00240 Helsinki, Finland*
[n] *MRC Centre for Environment and Health, Environmental Research Group, Imperial College London, United Kingdom*
[o] *NIHR HPRU in Environmental Exposures and Health, Imperial College London, United Kingdom*
[p] *Environment and Health Administration, SLB-analys, Box 8136, 104 20 Stockholm, Sweden*
[q] *ENRACT, Institute of Nuclear and Radiological Science & Technology, Energy & Safety, NCSR Demokritos, 15310 Ag. Paraskevi, Athens, Greece*
[r] *Department of Environment, CIEMAT, Madrid 28040, Spain*
[s] *Leibniz Institute for Tropospheric Research (TROPOS), Leipzig, Germany*
[t] *Saxon State Office for Environment, Agriculture and Geology (LfULG), Dresden, German*
[u] *Institute for Occupational, Social and Environmental Medicine, Medical Faculty, Heinrich-Heine-University of Düsseldorf, Germany*
[v] *Laboratoire des Sciences du Climat et de l'Environnement, CEA/Orme des Merisiers, 91191 Gif-sur-Yvette, France*
[w] *Institut National de l'Environnement Industriel et des Risques (INERIS), Parc Technologique Alata BP2, 60550 Verneuil-en-Halatte, France*
[x] *European Commission, Joint Research Centre (JRC), 21027 Ispra, Italy*
[y] *Institute of Atmospheric Sciences and Climate of National Research Council, ISAC-CNR, 73100 Lecce, Italy*
[z] *Finnish Meteorological Institute, Atmospheric Composition Research, Helsinki, Finland*
[aa] *Institute for Atmospheric and Earth System Research (INAR), Faculty of Science, University of Helsinki, Finland*
[bb] *Department of Public Health Sciences, University of Rochester School of Medicine & Dentistry, Rochester, NY 14642, USA*
[cc] *Department of Environmental Sciences, Faculty of Meteorology, Environment and Arid Land Agriculture, King Abdulaziz University, Jeddah, Saudi Arabia*

* Corresponding authors at: Institute of Environmental Assessment and Water Research (IDAEA-CSIC), 08034 Barcelona, Spain (M. Garcia-Marlès).
E-mail addresses: meri.garcia@idaea.csic.es (M. Garcia-Marlès), xavier.querol@idaea.csic.es (X. Querol).

https://doi.org/10.1016/j.envint.2024.108510
Received 22 December 2023; Received in revised form 1 February 2024; Accepted 16 February 2024
Available online 17 February 2024

ARTICLE INFO

Keywords:
Nanoparticles
Particle number concentrations
Air quality
Ambient air

ABSTRACT

Ultrafine particles (UFP, those with diameters ≤ 100 nm), have been reported to potentially penetrate deeply into the respiratory system, translocate through the alveoli, and affect various organs, potentially correlating with increased mortality. The aim of this study is to assess long-term trends (5–11 years) in mostly urban UFP concentrations based on measurements of particle number size distributions (PNSD). Additionally, concentrations of other pollutants and meteorological variables were evaluated to support the interpretations. PNSD datasets from 12 urban background (UB), 5 traffic (TR), 3 suburban background (SUB) and 1 regional background (RB) sites in 15 European cities and 1 in the USA were evaluated. The non-parametric Theil-Sen's method was used to detect monotonic trends. Meta-analyses were carried out to assess the overall trends and those for different environments. The results showed significant decreases in NO, NO_2, BC, CO, and particle concentrations in the Aitken (25–100 nm) and the Accumulation (100–800 nm) modes, suggesting a positive impact of the implementation of EURO 5/V and 6/VI vehicle standards on European air quality. The growing use of Diesel Particle Filters (DPFs) might also have clearly reduced exhaust emissions of BC, PM, and the Aitken and Accumulation mode particles. However, as reported by prior studies, there remains an issue of poor control of Nucleation mode particles (smaller than 25 nm), which are not fully reduced with current DPFs, without emission controls for semi-volatile organic compounds, and might have different origins than road traffic. Thus, contrasting trends for Nucleation mode particles were obtained across the cities studied. This mode also affected the UFP and total PNC trends because of the high proportion of Nucleation mode particles in both concentration ranges. It was also found that the urban temperature increasing trends might have also influenced those of PNC, Nucleation and Aitken modes.

1. Introduction

Atmospheric particulate matter (PM) is one of the main air pollutants (WHO, 2021a). It is estimated that ambient particulate air pollution caused 4.2 million premature deaths worldwide in 2019, as derived from the aggravation of cardiovascular and respiratory diseases, among others (WHO, 2021a). The nature and severity of the effects depend, among others, on the size of the particles. Therefore, air quality standards are set up for the ambient air mass concentrations of particles (μg m^{-3}) with aerodynamic diameters ≤10 μm (PM_{10}) and ≤2.5 μm ($PM_{2.5}$). However, a large fraction of the particles in the atmosphere are smaller than 100 nm (diameters can be as fine as 1 nm). These very fine particles contribute minimally to the PM mass concentrations but represent the bulk of the particle number concentrations (PNC, # cm^{-3}), which are not regulated by ambient air quality standards (Seinfeld and Pandis, 2016). Thus, when focusing on this aerosol size range, measurements are performed as PNC and not PM mass. PNC measurements are frequently derived from particle number size distribution (PNSD) by calculating PNCs for specific size ranges. Conventionally, the term ultrafine particles (UFP) is used for particles with a diameter ≤100 nm, while the Nucleation, Aitken and Accumulation size modes refer to particles in the <25, 25–100 and >100 nm size ranges, respectively (e.g., Seinfeld and Pandis, 2016; CEN, 2020; ISO, 2023). The term "nanoparticle" is usually used for manufactured particles, while "ultrafine" is outdoor or indoor aerosols of a similar size. Furthermore, because most of the total PNC is accounted for by UFPs in urban areas (84 ± 3.7 % as average and standard deviation of 27 datasets in Europe, Trechera et al., 2023), the terms PNC and UFP are used in many studies as equivalents. Thus, PNC and UFP are not actually equivalents, but PNC is used as a surrogate for true UFP.

It has been reported that the size of UFPs not only allows them to reach the deeper parts of the respiratory system but also to translocate through the alveoli and reach the circulatory system and from there any organ in the body (Oberdörster et al., 2005; Peters et al., 2006; Kreyling et al., 2014; Cassee et al., 2019). Furthermore, other studies also evidenced that there is translocation through the olfactory nerve in the nose into the brain, and UFP have been reported to cross cell membranes in ways other than phagocytosis (Oberdörster et al., 2004; Genc et al., 2012; among others). A number of studies found a positive relationship between exposure to UFP and increased premature mortality (e.g., Wichmann et al., 2000; Ibald-Mulli et al., 2004; Tobías et al., 2018; Schwarz et al., 2023). However, Ohlwein et al. (2019), US EPA (2019) and WHO (2021b) concluded that the epidemiological results of the health effects of UFP are inconsistent. This inconsistency might be due to different types of UFP prevailing in different regions, a lack of harmonization in UFP measurements, high exposure assignment error based on the high microscale variability in space and time of UFP concentrations, a lack of long-term time-series available to epidemiological studies, or a lack of actual widespread impacts on health (Cassee et al., 2019). Based on the above considerations, the last WHO Air Quality Guidelines did not set up specific guidelines for PNC (or UFP), but recommended the long-term measurements of these variables with harmonized measurement protocols to better evaluate the convenience of such specific guidelines for UFP (WHO, 2021b). Alternatively, CEN (2020), ACTRIS (2021), RI-URBANS (2022) and Trechera et al. (2023) suggest the measurement of total PNCs with at least a finer size detection limit of 10 nm (50 % efficiency) and PNSD measurements in the range of 10 to 800 nm. PNC in the range of <10 nm might be high, but measuring this fraction is complex, and it is also recommended by ACTRIS (2021) and RI-URBANS (2022) in areas where nucleation mode particles are expected to be high.

Shipping is the major source of PNC in Europe with around 8.2 10^{26} # yr^{-1} followed by road traffic with 4.3 10^{26} # yr^{-1}, and industry with 4.2 10^{26} # yr^{-1} (Kuenen et al., 2022). However, as occurs also for NO_2, the proximity of the urban population to road traffic emission accounts for a very high road traffic contribution to urban PNC exposures. Thus, studies on source apportionment of UFP point to road traffic as the main source in urban areas (Zhou et al., 2005; Pey et al., 2009; Dall'Osto et al., 2011; Harrison et al., 2011; Brines et al., 2014, 2015; Beddows et al., 2015, 2019; Rivas et al., 2020; Hopke et al., 2022). Traffic typically accounts for >70 % of the annual UFP emissions in urban environments (Hopke et al., 2022). In addition to road traffic, photochemical nucleation (leading to new particle formation), urban background (with a high load from traffic), regional background, long-range transport, harbours, airports, and domestic heating emissions have been reported to contribute to urban UFP concentrations. As it could be expected from its origin, photochemical nucleation is characterised by PNSD peaking at the finest sizes, followed by harbours and airports, typically with a prevailing Nucleation mode, see for example Rivas et al. (2020) and Stacey et al. (2020). Traffic exhaust emissions typically result in two major modes at 30–35 nm and 60–80 nm (Hopke et al., 2022), but also a major fraction of very small particles (smaller than 30 nm in diameter) (Trechera et al., 2023). The remaining aforementioned sources (urban and regional background, long range transport and domestic heating) are characterised by modes close to or coarser than 100 nm, according to the above references.

The few available studies analysing long term trends of UFP (e.g., Simon et al., 2020; Mikkonen et al., 2020; Presto et al., 2021; Chen et al., 2022; Damayanti et al., 2023) have found decreasing trends over the last two decades. Given that road traffic is the major source of urban UFP, these trends have been related to the reduction of particulate emissions from vehicle exhausts by the implementation of emission standards, especially EURO 5 and 6 (for cars) and V and VI (for heavy duty vehicles), and the equivalent TIER standards (2 and 3) in US, for which diesel particle filters (DPF) are required. The decrease of the sulfur content in the fuels of the vehicles might have also had an important impact in abating SO_2, and associated nucleation of particles (Chen et al., 2022), but this was already implemented in Europe before the period of this study. Damayanti et al. (2023) found that for a street canyon in London this effect was very evident for the Aitken and Accumulation modes, but the Nucleation one was largely unaffected. They proposed that the DPF do no retain semi-volatile organic compounds (SVOCs) emitted by diesel cars, and the nucleation of these SVOCs and the abatement of the condensation sink (CS) might account for the non-decreasing trend of the Nucleation mode. Furthermore, abrasion UFP are also emitted as part of the non-exhaust vehicle emissions (Dahl et al., 2006; Mathissen et al., 2011; Niemann et al., 2020; Li et al., 2023; and references therein).

Based again on the European emission inventory for the PNC-PNSD, 2018 emissions from diesel passenger cars reached 17.5 10^{25} # yr^{-1}, while emissions from petrol cars reached around 0.5 10^{25} # yr^{-1} (Kuenen et al., 2022). Furthermore, emissions of 9.8 10^{25} # yr^{-1}, and 13.5 10^{25} # yr^{-1} from (mostly diesel) light and heavy-duty vehicles have to be added. Thus, the diesel fleet is still responsible for a very large fraction of UFP emissions in Europe.

The implementation of major air quality measures and the EURO/TIER standards have also had an effect on the abatement of black carbon (BC) (Savadkoohi et al., 2023), and nitrogen dioxide (NO_2) and carbon monoxide (CO) (EMEP, 2016; ETC, 2020). Concentrations of SO_2 (mainly emitted by fossil fuel burning in Europe) drastically decreased as a consequence of deindustrialization and regulation measures implemented at European scale (EMEP, 2016). On the other hand, the concentrations of PM_{10} and $PM_{2.5}$ also decreased in 2000–2010 but a flat trend was recorded since then at many sites (EMEP, 2016; ETC, 2020). In contrast, concentrations of O_3 tend to increase in many urban environments due to the reduction of nitrogen oxides (NO_X) in a VOC-limited urban O_3 formation regime or to a steeper decrease of nitrogen monoxide (NO) versus NO_2 and the consequent lower titration of O_3 in environments without strong local O_3 formation (ETC, 2020; Sicard et al., 2021).

RI-URBANS (Research Infrastructures Services Reinforcing Air Quality Monitoring Capacities in European Urban & Industrial Areas, the European Union's Horizon 2020 research and innovation program, contract 101036245) is a European research project, which demonstrates the applications of advanced air quality service tools in urban Europe to improve the assessment of air quality policies, including a better evaluation of health impacts. In this context, this study aims to gather and evaluate available long-term trends of UFP and different particle size modes, based on PNSD data obtained at 21 (mostly urban) sites from 15 urban areas in Europe (11 member states) and one from the USA. A prior RI-URBANS study (Trechera et al., 2023) reported the phenomenology of UFP in urban Europe and compared the 2017–2019 concentrations across different cities and environments. Additional work is ongoing on the source apportionment of PNSD for 23 (mostly urban) sites using receptor modelling tools. In the current study we evaluate and interpret the trend analyses of the above 21 datasets for a period covering up to 11 years (2009–2019). A number of sites cover a shorter period of time, but in all cases, at least the last 5 years of measurement are available. The years 2020–2022 are intentionally excluded to avoid interferences of the COVID19-lockdown effects. To support interpretations, we also evaluate compiled datasets of conventional pollutants (BC, NO_2, NO, CO, SO_2, O_3, PM_{10}, $PM_{2.5}$ and PM_1) and meteorological variables (temperature, T; relative humidity, RH; atmospheric pressure, P; wind speed, WS; solar radiation, RAD; and rain, R) concurrently measured with the PNSDs.

2. Methodology

2.1. Cities and sites providing UFP-PNSD data

This study is based on 5 to 11 years UFP-PNSD datasets from the period 2009–2019 compiled by RI-URBANS and supplied from advanced air quality monitoring networks and research sites. The selection of sites for this study is based upon a previous study on the phenomenology of UFP in urban Europe by Trechera et al. (2023), allowing coverage of all ranges of concentrations of urban pollutants in cities from regions with different climate patterns, emission volume and sources and urban morphologies. These include (see Fig. 1 and Table 1):

- Twelve urban background (UB) sites covering most of Europe: Athens (ATH_UB), Barcelona (BCN_UB), Budapest (BUD_UB), Dresden (DRE_UB), Helsinki (HEL_UB), Lecce (LEC_UB), Leipzig (LEI_UB), London (LND_UB), Madrid (MAD_UB), Mülheim (MUL_UB), Zurich (ZUR_UB), and Rochester (ROC_UB) in New York State in US.
- Five traffic (TR) sites in Central (C), West (W) and North (N) Europe: Dresden (DRE_TR), Helsinki (HEL_TR), Leipzig (LEI_TR), London (LND_TR) and Stockholm (STO_TR); but not TR sites in South (S) Europe.
- Three suburban background (SUB) sites and one regional background (RB): Athens (ATH_SUB), Paris (PAR_SUB) and Prague (PRA_SUB); the regional background of Ispra (IPR_RB).

Thus, in total, 21 sites provided at least 5 years of hourly data in the period 2009–2019 of UFP-PNSD for this study. The period was selected excluding 2020–2022 to avoid the effects of the decrease of pollution due to the COVID19-lockdown, which were variable across urban Europe (Salma et al., 2020; Dinoi et al., 2021; Eleftheriadis et al., 2021; Petit et al., 2021; Putaud et al., 2021 and 2023). All the PNSD data used in this study is openly available in the EBAS database infrastructure (https://ebas.nilu.no/). Data corresponding to co-located measurements of other pollutants (BC, NO_2, NO, CO, SO_2, O_3, PM_{10}, $PM_{2.5}$ and PM_1) and meteorological variables (T, RH, P, WS, RAD and R) were also collected, when available, from the same sites or nearby air quality monitoring sites. Table S1 summarises the hours/year of UFP-PNSD measurements included in this study for each site.

2.2. Instrumentation and measurements

PNSD datasets were obtained from different types and models of Mobility Particle Size Spectrometer (MPSS), reported in Table 2. Concentrations of BC, PM and gaseous pollutants, and meteorological variables were collected from each site by instrumentation fulfilling European standards. All the data were averaged to hourly values.

Since different instruments were used to obtain PNSD datasets, the measured size ranges varied. Following ACTRIS and CEN guidance, it is suggested to measure the total PNCs with at least a finer size detection limit of 10 nm, and the recommended size measurement range for PNSD is 10–800 nm. As reported in Trechera et al. (2023), several sites start size measurements from 11 to 17 nm (BCN_UB, BUD_UB, HEL_TR, LND_UB, LND_TR, MAD_UB, MUL_UB, PAR_SUB, ROC_UB and ZUR_UB), instead of the recommended 10 nm, or end with lower coarser sizes from 410 to 794 nm (ATH_UB, ATH_SUB, BCN_UB, LND_UB, LND_TR, MAD_UB, MUL_UB, PAR_SUB, PRA_SUB, ROC_UB, STO_TR, and ZUR_UB), instead of the recommended 800 nm. The latter does not have a big impact to the total PNC because of the relatively low PNC within the coarser sizes. However, the lower size detection limit affects to a much higher degree the total PNC, and especially the Nucleation mode concentrations. Thus, when comparing PNSD concentrations from all

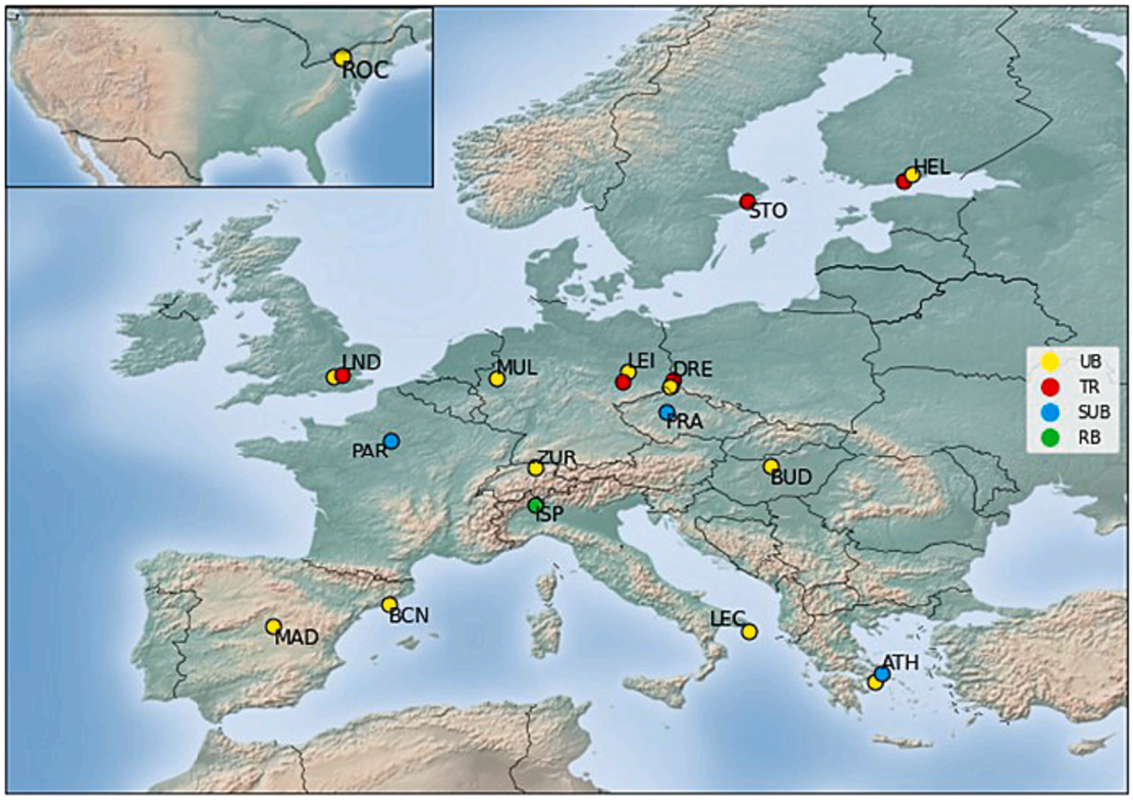

Fig. 1. Location of the cities and type of station supplying data on PNC and PNSD. UB, Urban background; TR, Traffic; SUB, Suburban background; RB, Regional background.

sites, the lower size detection limits have to be considered.

In this study, trend analyses are carried out for UFP ($N_{10\text{-}100}$), PNC ($N_{10\text{-}800}$) and the Nucleation (N), Aitken (A) and Accumulation (Ac) modes ($N_{10\text{-}25}$, $N_{25\text{-}100}$ and $N_{100\text{-}800}$, respectively); and also, for the ancillary data (regulated atmospheric pollutants and meteorological parameters).

2.3. Data treatment and trend analysis

Data treatment and statistical analysis were carried out using R statistical software (v4.2.3, R Core Team, 2023) and the *Openair* package (Carslaw and Ropkins, 2012) in R.

Data series with periods exceeding 3 years were evaluated to detect monotonic trends over the time using the non-parametric Theil-Sen method (Sen, 1968; Theil, 1992). This method, robust against outliers, is commonly applied for air quality data analysis (Carslaw and Ropkins, 2012). To this end, monthly aggregation of data series was performed with a threshold of 30 % of the hourly concentration data. The selection of a 30 % threshold was based on the data availability considering the amount of data used in the study. Many sites had data availability of

Table 1
List of air quality sites supplying UFP-PNSD datasets to this study with location, type of environment and period of measurement. Coord., Coordinates; Alt., Altitude; UB, Urban Background; TR, Traffic; SUB, Suburban Background; RB, Regional Background.

City (Country)	Station Name	Station type	Acronym	Coord.; (Alt., m a.s.L.)	Period
Athens (GR)	Thissio	UB	ATH_UB	38.00 N, 23.72 E; (110)	2015–2019
Barcelona (ES)	Palau Reial	UB	BCN_UB	41.39 N, 2.13E; (80)	2013–2019
Budapest (HU)	BpART	UB	BUD_UB	47.48 N, 19.06 E; (115)	2013–2019
Dresden (DE)	Winckelmann Str.	UB	DRE_UB	51.04 N, 13.73 E; (120)	2010–2019
Helsinki (FI)	SMEAR III	UB	HEL_UB	60.12 N, 24.58 E; (26)	2009–2019
Lecce (IT)	ECO Observatory	UB	LEC_UB	40.20 N, 18.07 E; (50)	2015–2019
Leipzig (DE)	TROPOS	UB	LEI_UB	51.35 N, 12.43 E; (113)	2009–2019
London (GB)	North Kensington	UB	LND_UB	51.52 N, 0.21 W; (27)	2009–2018
Madrid (ES)	CIEMAT-Moncloa	UB	MAD_UB	40.45 N, 3.73 W; (669)	2009–2019
Mülheim an der Ruhr (DE)	Mülheim-Styrum	UB	MUL_UB	51.45 N, 6.87 E; (39)	2009–2019
Rochester NY (US)	NYS DEC	UB	ROC_UB	43.15 N, 77.55 W; (137)	2009–2019
Zurich (CH)	Kaserne	UB	ZUR_UB	47.38 N, 8.53 E; (410)	2015–2019
Dresden (DE)	North	TR	DRE_TR	51.07 N, 13.74 E; (116)	2009–2019
Helsinki (FI)	Mäkelänkatu	TR	HEL_TR	60.19 N, 24.95 E: (26)	2015–2019
Leipzig (DE)	Mitte	TR	LEI_TR	51.34 N, 12.38 E; (111)	2010–2019
London (GB)	Marylebone Rd	TR	LND_TR	51.52 N, 0.15 W; (35)	2010–2019
Stockholm (SE)	Hornsgatan	TR	STO_TR	59.32 N, 18.05 E; (20)	2010–2018
Athens (GR)	Demokritos	SUB	ATH_SUB	37.99 N, 23.82 E; (270)	2010–2019
Paris (FR)	SIRTA	SUB	PAR_SUB	48.71 N, 2.16 E; (162)	2012–2019
Prague (CZ)	Suchdol	SUB	PRA_SUB	50.13 N, 14.38 E; (277)	2012–2019
Ispra (IT)	JRC	RB	IPR_RB	45.80 N, 8.63 E; (209)	2009–2019

Table 2
Instrumentation used to measure UFP-PNSD, size range of measurement and ancillary data available in each site of the study. ND, Not-determined; SMPS, Scanning Mobility Particle Sizer; CPC, Condensation Particle Counter; MAAP, Multi-Angle Absorption Photometer; DMPS, Differential Mobility Particle Sizer; TSMPS, Twin Scanning Mobility Particle Sizer; DMA, Differential Mobility Analyser; TDMPS, Twin Differential Mobility Particle Sizer; UCPC, Ultrafine Condensation Particle Counter; OPC, Optical Particle Counter.

Station	UFP-PNSD instrumentation	Range (nm)	Ancillary data
ATH_UB	SMPS TSI 3034	10.4–487	BC, NO, NO_2, O_3, CO, T, RH, P, RAD, R
BCN_UB	SMPS TSI 3080 + CPC TSI 3772	12.2–478.3	BC, PM10, PM2.5, PM1, SO_2, N, NO_2, O_3, CO, T, RH, P, RAD, WS
BUD_UB	DMPS + CPC TSI 3775	10.8–816.2	PM10, SO_2, NO, NO_2, O_3, CO, T, RAD
DRE_UB	TROPOS-SMPS uses a Vienna-type DMA 28 cm + CPC TSI 3772	10–800	BC, PM10, SO_2, NO, NO_2, O_3, T, RH, P, RAD, WS, R
HEL_UB	TDMPS Hauke-type DMA 10.9 cm + CPC TSI 3025/3756 and Hauke-type DMA 28 cm + CPC 3010/3772	10–794	SO_2, NO, NO_2, O_3, CO, T, RH, P, RAD, WS
LEC_UB	TROPOS-SMPS uses a Vienna-type DMA 28 cm + CPC TSI 3772	10–800	BC, SO_2, NO, NO_2, O_3, T, RH, RAD, WS, R
LEI_UB	TROPOS-TDMPS uses Vienna-type DMAs 11 and 28 cm + CPC TSI 3025/3010	10–800	ND
LND_UB	SMPS TSI 3080 + CPC TSI 3775 with long DMA	17–604	BC, PM10, PM2.5, SO_2, NO, NO_2, O_3, CO, T, RH, WS
MAD_UB	SMPS TSI 3080L + CPC TSI 3775	15.1–661.2	BC, PM10, PM2.5, SO_2, NO, NO_2, O_3, CO, T, RH, RAD, WS, R
MUL_UB	SMPS TSI 3080 + CPC TSI 3772	14.1–495.8	PM10, PM1, NO, NO_2, T, RH, RAD, WS, R
ROC_UB	SMPS TSI 3071 + CPC TSI 3010	11.1–469.8	BC, PM2.5, SO_2, NO, NO_2, O_3, T, RH, WS
ZUR_UB	SMPS TSI 3034 + Nafion aerosol dryer	16.8–478.3	BC, PM10, SO_2, NO, NO_2, O_3, CO, T, RH, P, RAD, WS, R
DRE_TR	TROPOS-TSMPS uses Vienna-type DMAs 11 and 28 cm + CPC TSI 3025/3010	10–800	BC, PM10, NO, NO_2, O_3, T, RH, P, RAD, WS
HEL_TR	UHEL DMPS Vienna-type DMA + CPC Airmodus A20	11–800	BC, PM10, PM2.5,, NO, NO_2, O_3
LEI_TR	TROPOS-TDMPS uses Vienna-type DMAs 11 and 28 cm + CPC TSI 3025/3010	10–800	BC, PM10, SO_2, NO, NO_2, T, RH, RAD, WS, R
LND_TR	SMPS TSI 3080 + CPC TSI 3775 with long DMA	16.6–604.3	BC, PM10, PM2.5, SO_2, NO, NO_2, O_3, CO
STO_TR	DMPS Stockholm university handmade + CPC TSI 3010/3775	10–410	PM10, PM2.5, PM1, NO, NO_2, CO, T, RH, P, RAD, WS, R
ATH_SUB	SMPS TSI 3080 + CPC TSI 3772	10–550	PM10, PM2.5, NO, NO_2, O_3, T, RH, RAD, R
PAR_SUB	SMPS GRIMM 5416 + OPC GRIMM	10.9–791.5	BC, PM1, NO, NO_2, O_3, CO, T, RAD, WS
PRA_SUB	SMPS TSI 3034 rebuilt at TROPOS	10.3–519.4	PM10, PM2.5, SO_2, NO, NO_2, O_3, CO
IPR_RB	DMPS Vienna-type, home-made + CPC TSI 3010/3772	10–800	BC, PM10, SO_2, NO, NO_2, O_3, CO, RH, P, RAD, R

<50 % due to the complexity of UFP-PNSD measurements and the need of frequent instrumentation maintenance, as it is evidenced by Trechera et al. (2023). For instance, Chen et al. (2022) established a threshold of 40 %. In this study, we tried to do the trends with different thresholds of data availability and considered 30 % was the most suitable in order to have representativity of the data without losing too many months of data.

The magnitude of the trends was quantified by the Theil–Sen slope, which is the median of all the possible slopes between the data pairs and the statistical significance (ss) was also evaluated. Due to the relatively extensive temporal gaps, de-seasonalisation using Seasonal Decomposition of Time Series by Loess (Cleveland et al., 1990) was not applied. These analyses were conducted using the Openair package. It should be noted that some of the time series are relatively short for the discernment of trends, and some of the longer time series show different gradients dependent upon the time interval selected.

The individual slopes, expressed as a percentage change per year with their 95 % confidence interval, were summarised using random-effects meta-analysis due to the large heterogeneity of the data between the included sites (Chen and Peace, 2013). The mean effect was calculated for each class of site individually (urban, suburban, regional and traffic sites) as well as globally to provide a comprehensive overview of the results. Meta-analyses were carried out using the "meta" R package version 6.5–0 (Balduzzi et al., 2019).

3. Results

3.1. Pollutants related with road traffic

NO_2 decreased at all sites with a ss trend with the exception of ATH (UB and SUB), in which increasing trends were recorded (+2.64, 95 %CI = [−3.68;7.88] and + 2.70, 95 %CI = [0.06;6.84] % yr^{-1}, respectively), and LEC_UB and ROC_UB, with non-ss decreasing trends (Fig. 2). The largest ss decreases were recorded for IPR_RB, HEL_TR and HEL_UB (−18.91 [−24.13;-15.00], −8.58 [−10.14;-6.85] and −6.01 [−6.97;-4.83] % yr^{-1}, respectively). Taking all the SUB sites the meta-analysis yielded a non-ss trend, while for all UB and TR sites there were marked ss decreasing trends of −3.11 [−4.01;-2.22] and −3.81 [−6.03;−1.59] % yr^{-1}, respectively. For NO, trends were very similar to those described for the type of environment, with only a non-ss increase in LEC_UB, and ss decreases in most of the other sites (Fig. 2). In this case the meta-analysis showed ss decreasing trends for SUB, UB and TR sites (−4.34 [−6.09;-2.58], −3.75 [−4.87;-2.64] and −4.75 [−8.37;-1.14] % yr^{-1}, respectively).

BC decreased at all sites with ss trends with the exception of ATH_UB and LEC_UB, in which non-ss decreasing trends were recorded. The highest decrease again being at HEL_TR (−9.14 [−11.53;-6.80]. HEL_UB does not have a long record for this parameter (Fig. 2). The meta-analysis showed ss decreasing trends for UB and TR sites, with −4.55 [−5.84;-3.27] and −7.42 [−8.62; −6.22] % yr^{-1}, respectively. Thus, the slope increases with the approach to the TR sites.

CO decreased at all sites with ss trends with exception of BCN_UB and ZUR_UB (with non-ss decreasing trends), and BUD_UB (with a non-ss increment) (Fig. 2). The highest decrease was recorded again (as for NO_2) in IPR_RB (−19.49 [–22.77;-17.33] % yr^{-1}), followed by ATH_UB and LND_TR (−6.14 [−11.47;-0.15] and −5.37 [−5.66;-5.02] % yr^{-1}, respectively). The meta-analysis showed ss decreasing trends for SUB, UB and TR sites, with −4.74 [−5.57;-3.91]; −2.36 [−3.48;-1.23] and −4.49 [−6.27;-2.71] % yr^{-1}, respectively.

3.2. Other pollutants

PM_{10} decreased with ss trends at 10/15 sites, and the meta-analysis yielded ss trends for SUB (−4.66[−6.22;-3.11] % yr^{-1}), UB (−2.21 [−3.08;-1.34] % yr^{-1}) and TR (−3.81 [−4.25;-3.37] % yr^{-1}) sites (Fig. 3). Similar dominant ss decreasing trends were observed for $PM_{2.5}$ (5/9 sites), with ss decreasing trends for the averages of SUB (−2.91 [−4.13;-1.70] % yr^{-1}), UB (−1.86 [−3.33;-0.39] % yr^{-1}) and TR (−3.72 [−5.95;-1.48] % yr^{-1}) sites (Fig. 3). For PM_1 only 4 sites provided long datasets and the meta-analysis only yielded a ss decreasing trend for IPR_RB (Fig. 3).

O_3 decreased with a ss trend only at ATH_UB (−10.14 [−12.80;-3.78] % yr^{-1}) and close to ss at BCN_UB (Fig. 4). It increased at all TR sites, with an average rate of + 2.65 [0.56;4.74] % yr^{-1}; but the meta-analysis yielded non-ss trends at UB and SUB sites.

SO_2 drastically decreased in 1990–2015 (Aas et al., 2019), but it

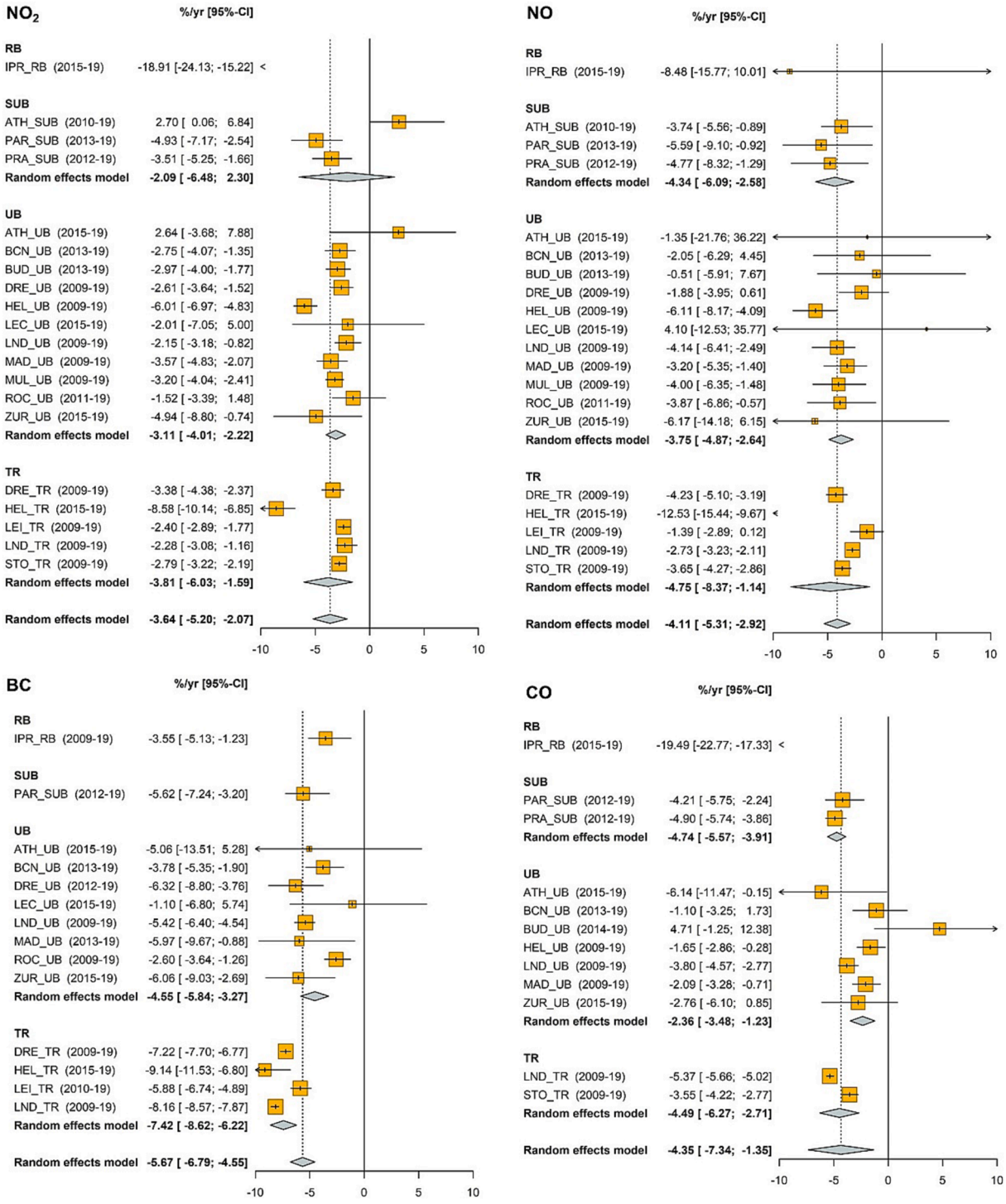

Fig. 2. Results of the trend analysis and subsequent meta-analysis for NO_2, NO, BC and CO datasets. Trends are calculated using the Theil-Sen method. Results of the meta-analysis are presented globally for each pollutant and for the different site categories (UB, TR, SUB, and RB). The dashed lined represents the global meta-analysis. Random effects model: mean effect calculated for each type of site.

continued decreasing in the analysed period. The decreases were ss at 9/13 sites (Fig. 4). The meta-analysis yielded a ss decreasing trend of −5.59 [−8.54;-2.63] % yr^{-1}, considering all sites.

3.3. Ultrafine particles

PNC decreased with ss trends at 9/21 sites (from central and north Europe, UK, USA and the regional background site in Italy) (Fig. 5). The meta-analysis yielded a non-ss trend for SUB sites, but ss for UB (−1.89 [−3.70;-0.09] % yr^{-1}), TR (−5.13 [−7.71;-2.56] % yr^{-1}) sites, and including all sites (−2.46 [−3.89;-1.04] % yr^{-1}). As it could be expected, UFP trends were similar to that of PNC, with ss decreases at 8/21 sites (the same as before but excluding HEL_TR), and only a ss increase in BUD_UB (Fig. 5). The meta-analysis again yielded a non-ss trend for the SUB sites, but in this case, for the UB sites as well. The ss decreasing trends were only seen in this case for the TR (−4.50 [−7.41;-1.59] % yr^{-1}) sites, and the global meta-analysis (−1.98 [−3.45;-0.52] % yr^{-1}). These results showed larger decreasing PNC and UFP slopes in the TR

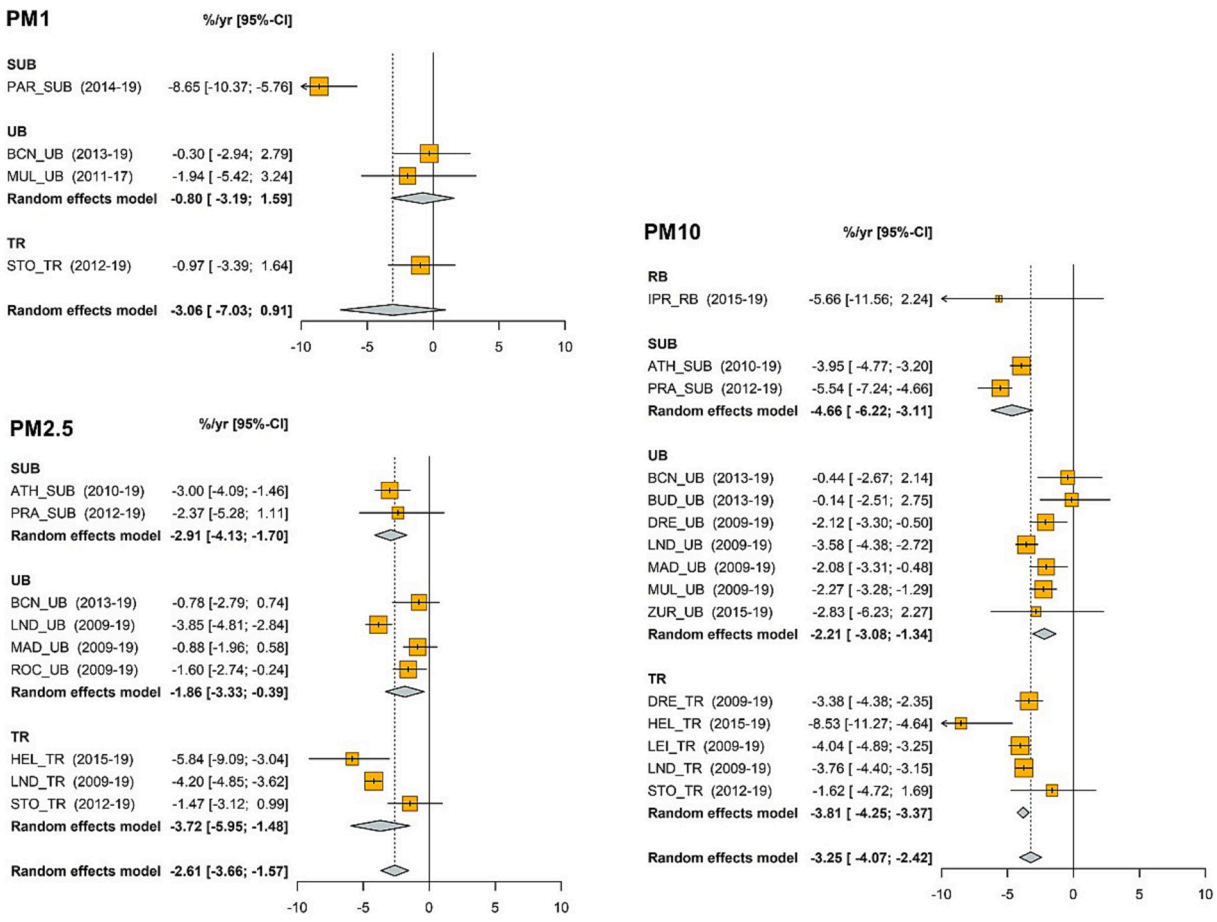

Fig. 3. Results of the trend analysis and subsequent meta-analysis for PM_1, $PM_{2.5}$ and PM_{10} datasets. Trends are calculated using the Theil-Sen method. Results of the meta-analysis are presented globally for each pollutant and for the different site categories (UB, TR, SUB, and RB). The dashed lined represents the global meta-analysis. Random effects model: mean effect calculated for each type of site.

sites compared with the UB ones, as also observed for the decreasing trends of the traffic-related pollutants. At IPR_RB, both PNC and UFP followed ss decreasing trends (−1.68 [−3.01;-0.28] and −1.27 [−2.04;-0.23] % yr^{-1}). For the UB and TR sites the slopes described above are equivalent to a decrease of −127 and −671 # cm^{-3} yr^{-1} for PNC and −60 and −491 # cm^{-3} yr^{-1} for UFP.

Trends for the Nucleation mode were similar to those of UFP with ss decreases at 6/21 sites (all of them from UK, central and north Europe), and ss increases at 5/21 sites (from southern and eastern Europe, but also ROC_UB, LND_UB and LEI_TR) (Fig. 6). The meta-analysis yielded non-ss decreasing trends for the SUB and TR sites and a non-ss increasing trend for UB sites. The percentage of Nucleation mode particles in PNC (N/PNC) followed ss decreasing trends at only 1/21 sites, while ss increasing trends were found at 9/21 sites. At 5/21 sites, non-ss increasing trends were found (Fig. 6). The meta-analysis yielded a ss decreasing trend for the SUB sites (−2.25 [−3.62;-0.87] % yr^{-1}), but a positive one for the UB sites (+3.14 [1.28;5.00] % yr^{-1}). For the TR sites, only STO_TR demonstrated a non-ss decreasing trend, while the other 4 sites followed positive ones. The meta-analysis showed an increasing trend (close to the ss) for TR sites (+1.60 [−0.31;3.50] % yr^{-1}).

The Aitken mode presented dominant ss decreasing trends, with ss decreases at 11/21 sites and a ss increase only in PRA_SUB (Fig. 6). The meta-analysis yielded a non-ss trend for the SUB sites, but ss ones for UB (−2.40 [−3.84;-0.96] % yr^{-1}) and TR (−5.79 [−8.11;-3.48] % yr^{-1}) sites, and including all sites (−2.81 [−4.26;-3.48] % yr^{-1}).

The Accumulation mode trends were similar to that of the Aitken mode, with ss decreases in 14/21 sites (Fig. 6). The meta-analysis yielded ss decreasing trends for UB (−3.69 [−4.98;-2.39] % yr^{-1}) and TR (−5.79 [−6.83;-4.75] % yr^{-1}) sites, and also including all sites (−3.92 [−4.99;-2.86] % yr^{-1}). IPR_RB followed also a ss decreasing trend of (−2.39 [−4.10;-0.42] % yr^{-1}), but SUB sites followed a non-ss one.

3.4. Meteorological variables

Fig. S23 summarises the results of the meta-analysis for the trend analyses of T, RH, P, WS, RAD and R. The results yielded ss increasing trends for T in urban Europe with a slope of 0.13 [0.09;0.18] °C yr^{-1}. In this study, 10/14 cities had ss T increases, 3/14 cities non-ss increases, and 1/15 city recorded near constant temperatures. The highest T increases were obtained for Dresden (TR site) and Leipzig with 0.33 [0.25;0.41] and 0.22 [0.13;0.31] °C yr^{-1}, respectively. Barcelona, Helsinki, Lecce, London, Mulheim, Paris, Stockholm and Zurich had increasing slopes of 0.13–0.19 °C yr^{-1}. These higher increases of T are taking place mostly in northern and central European cities, while those from southern and eastern Europe and the one from northern USA, have relatively lower slopes of increase.

The meta-analysis of the trends yielded also a ss slight increase of RAD, with 0.65 [0.15;1.15] % yr^{-1}, without major regional differentiations. The other four meteorological parameters evaluated did not provide ss trends and in most cases, the slopes were close to 0.

3.5. Analysis by city

The analysis by city is shown in Supplementary Figs. S1–S22 and

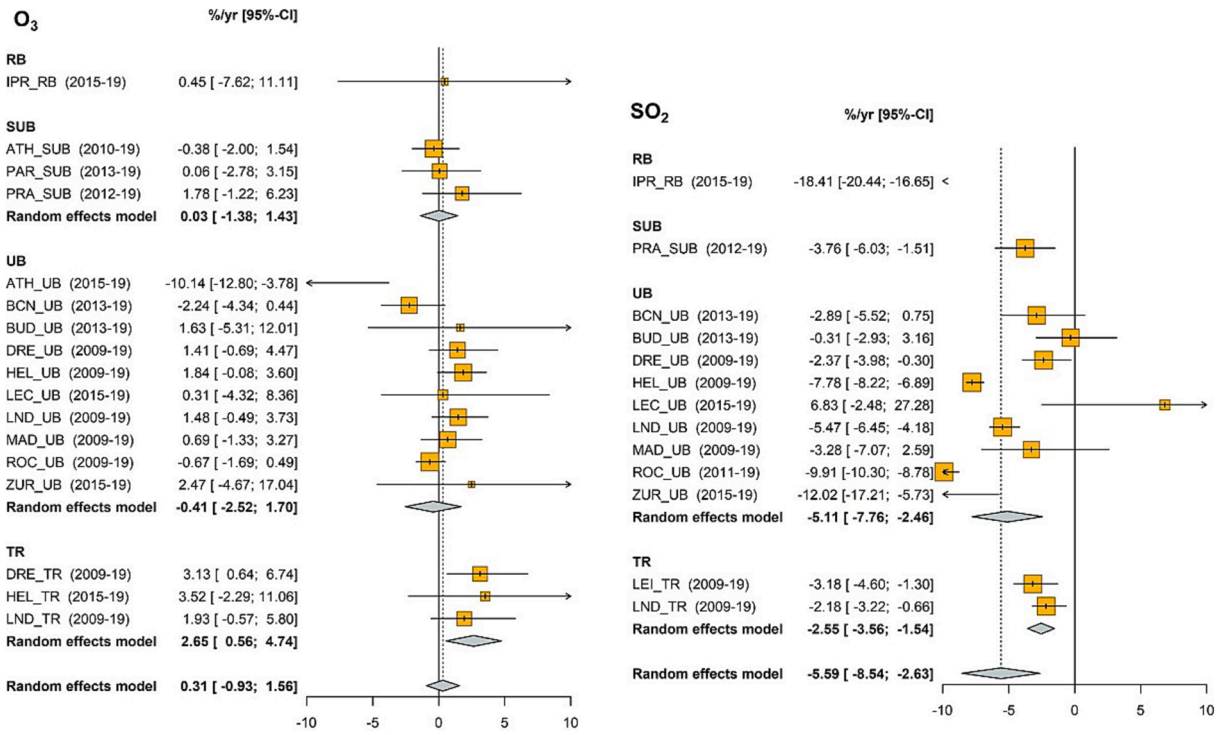

Fig. 4. Results of the trend analysis and subsequent meta-analysis for O_3 and SO_2 datasets. Trends are calculated using the Theil-Sen method. Results of the meta-analysis are presented globally for each pollutant and for the different site categories (UB, TR, SUB, and RB). The dashed lined represents the global meta-analysis. Random effects model: mean effect calculated for each type of site.

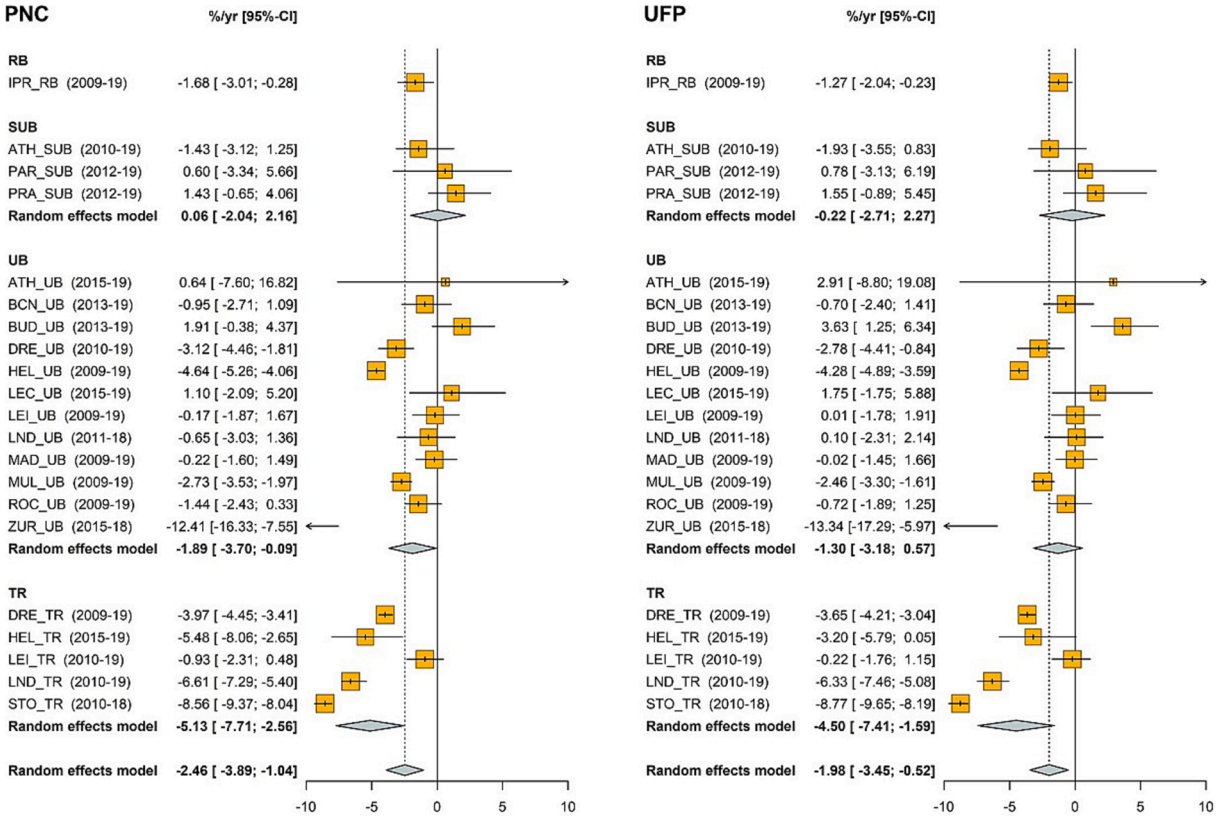

Fig. 5. Results of the trend analysis and subsequent meta-analysis for PNC and UFP datasets. Trends are calculated using the Theil-Sen method. Results of the meta-analysis are presented globally for each pollutant and for the different site categories (UB, TR, SUB, and RB). The dashed lined represents the global meta-analysis. Random effects model: mean effect calculated for each type of site.

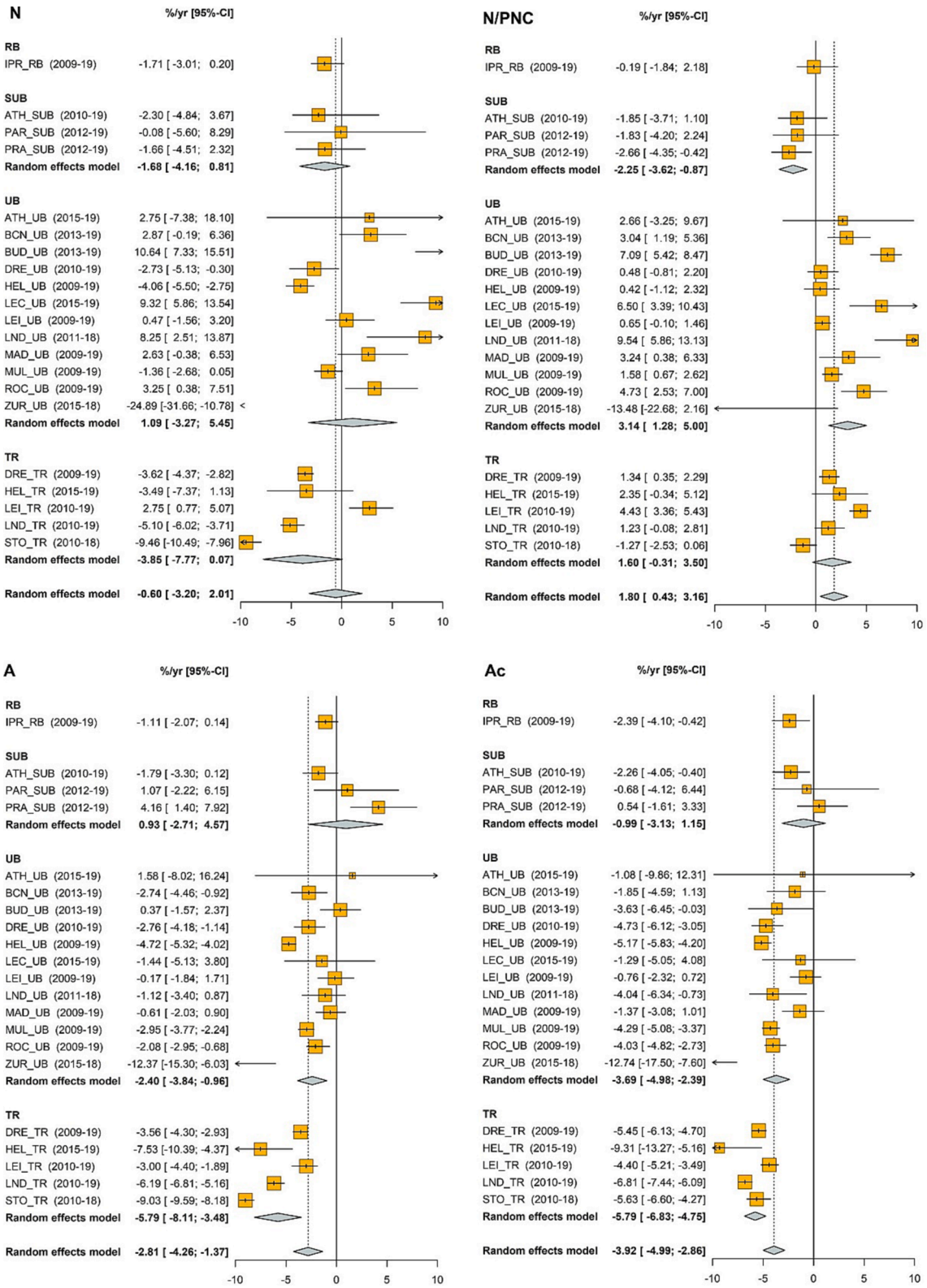

Fig. 6. Results of the trend analysis and subsequent meta-analysis for Nucleation mode (N), percentage of Nucleation mode particles in PNC (N/PNC), Aitken mode (A) and Accumulation mode (Ac) datasets. Trends are calculated using the Theil-Sen method. Results of the meta-analysis are presented globally for each pollutant and for the different site categories (UB, TR, SUB, and RB). The dashed lined represents the global meta-analysis. Random effects model: mean effect calculated for each type of site.

interpreted in Supplementary text T1.

4. Discussion

4.1. Trends of NO, NO_2, BC, CO, PM, O_3 and SO_2

Very similar NO_2 declines were found at all site types, consistent with the lower emissions of NO_X from EURO 6/VI diesel vehicles. For NO, there was also a decreasing trend at the vast majority of cities, consistent with NO_2 concentrations and declining emissions of traffic-related NO_X. Trends in NO were generally steeper than trends in NO_2 (21 % and 25 % higher for NO for UB and TR sites). This steeper NO decrease might be attributed to the progressively lower NO/NO_2 emission rates from the diesel vehicles in the last decade (Carslaw et al., 2016). A higher-than-average downward NO_2 trend at HEL (both UB and TR sites) and an upward trend in ATH (at both UB and SUB sites) were observed, while ATH (both UB and SUB sites) showed a NO decrease. This unusual behaviour in both sites in Athens might be explained by the increase of diesel cars between 2012 and 2015, which their circulation was banned in Athens before 2012, and diesel cars are higher NO_2 emitters than gasoline cars (Degraeuwe et al., 2017). Thus, from 2012 onwards and with a gradual increase, diesel cars started contributing with primary NO_2 emissions changing the photochemical balance of $NO/NO_2/O_3$. LEC_UB had a NO increasing trend, but that was non-ss. Although EURO 5/V vehicles beginning in 2011 were equipped with DPF, the impact of the higher-than-expected NO_X emissions from diesel vehicles (Anenberg et al., 2017) resulted in delayed impacts of the EURO 5/V and 6/VI standards in abating ambient air NO_2 (Grange et al., 2020; Benavides et al., 2021). The marked decrease of NO/NO_X ratios from vehicle emissions (according Carslaw et al. (2016) EURO 6 diesel cars emitted 67 % NO in NO_X, while in EURO 3 ones this proportion reached 91 %), and the delayed decrease of NO_2 from diesel vehicles (according the same study, EURO 2 diesel passenger cars emitted 0.08 g/km, while EURO 4 and early EURO 6 ones reached 0.33 and 0.14 g/km, respectively, in real world driving conditions) are probably the main causes of the differences in the slopes.

Downward ss BC trends were observed for all sites except LEC_UB and ATH_UB. These trends were consistent with the increased proportion of diesels with a DPF required by EURO 5/V (Damayanti et al., 2023). This decreasing trend was steeper than for NO_2 and NO (46 and 95 % higher than for NO_2, for UB and TR sites, respectively). LEC_UB appears to have experienced increased diesel traffic. ROC_UB (US) showed a smaller decline in BC, probably due to fewer light-duty diesel vehicles in the USA. Wood burning may also contribute to BC in some of the study sites, but Savadkoohi et al. (2023) reported that in most cases >75 % of the urban BC arises from road traffic. Furthermore, home heating and restaurants are additional urban sources (Yu et al., 2019).

The majority of sites followed a ss downward CO trend (BCN_UB and ZUR_UB are non-ss), probably associated with the growth of diesel share in the last decade and the lower emissions of the petrol vehicles since EURO 4 (ICCT, 2016). Thus, since 2006 (EURO 4) passenger diesel vehicles are allowed to emit only 0.50 g/km, and the petrol ones 1 g/km, while EURO 2–3 vehicles were allowed to emit 1.0–0.7 and 2.2–2.3 g/km, respectively (ICCT, 2016). These decreasing slopes were similar to those of NO_2 and NO, and were also attributed to decreased CO from road traffic. However, BUD_UB followed an upward trend similar to NO, possibly reflecting increased road vehicular activity affecting the site and might be also affected by the increased mean age of the passenger car fleet in Hungary (Mikkonen et al., 2020). ATH_UB followed a larger than average decline, suggesting a shift from gasoline to diesel vehicles, or possibly declining biomass combustion.

Downward trends were observed at all sites for $PM_{2.5}$ (but these were non-ss for PRA_SUB, BCN_UB, MAD_UB and STO_TR). These reductions were likely the result of reduced diesel exhaust emissions, and a decline of secondary inorganic aerosol precursors (EMEP, 2016, among others). The cause of the smaller reduction at BCN_UB is unknown. Among possible causes, one possibility is the marked increase of cruise and container ship traffic (Port de Barcelona, 2023). In STO_TR, $PM_{2.5}$ is mostly from long range transport from other countries. As expected, PM_{10}, which typically contains a high proportion of $PM_{2.5}$, followed a similar trend at most sites. Important contributors to PM_{10}, mostly in the $PM_{2.5\text{-}10}$ fraction, are the non-exhaust vehicle emissions (vehicle wear) and road dust, which increased in their relative contributions at TR sites (Amato et al., 2016). Hence, most sites showed decreasing PM_{10} trends. BCN_UB, BUD_UB, ZUR_UB and STO_TR showed limited and non-ss decreases. Possible reasons are associated with increased road traffic, and in the case of BCN, increased Saharan dust incursions or greater surface dryness facilitating road dust and soil resuspension. In the case of STO_TR, PM_{10} could be largely associated with non-exhaust particles from road wear, then the small non-ss decreasing trend might be due to the meteorology that affects the wetness of the roads in winter.

A small increase of O_3 at the majority of sites was consistent with lower NO_X emissions, and lower O_3 titration by NO. The increasing trends might be attributed to the higher decreasing slope of NO compared with that of NO_2, which reduces the O_3 titration potential (Colette et al., 2011; Escudero et al., 2014; Monks et al., 2015, among others). ATH_UB and BCN_UB followed decreasing O_3 trends. In ATH_UB these trends were consistent with increased NO_2, but not so in BCN_UB.

SO_2 decreasing trends were observed for most sites except LEC_UB, and were ss at most locations. These declines likely resulted from the reduced combustion of high S-fuels, such as coal and residual fuel oil (Crippa et al., 2016).

4.2. Trends of ultrafine particles and size fractions

PNC decreased with ss trends at 43 % of the sites (central and north Europe). The meta-analysis yielded a non-ss decreasing trend for SUB sites, but ss trends for UB and TR sites. For UFP, a similar pattern was found, but the ss decreasing trend was only observed at TR sites (−4.50 % yr^{-1}) and slightly lower than for PNC (−5.13 % yr^{-1}). Thus, dominant PNC and UFP decreases were observed, with higher slopes at the TR sites (171 % steeper in TR sites compared with the UB for PNC). These results suggest the effectiveness of DPF in abating the emissions and urban ambient concentrations of BC, PNC and UFP (Damayanti et al., 2023).

The Nucleation mode fraction followed very different trends among the evaluated cities. Several of them increased, most probably linked to a reduction in condensation sink potential, which facilitates new particle formation (McMurry and Friedlander, 1979; Spracklen et al., 2010; Kulmala et al., 2017). Others followed a decline, most notably STO_TR and LND_TR. The percentage of Nucleation mode particles in PNC (N/PNC) followed ss decreasing trends at only 5 % of the sites, while ss increasing trends were found at 43 % of the sites, and non-ss increasing trends at 29 %. At SUB sites, both Nucleation concentrations and percentage of Nucleation in PNC showed decreasing trends. These decreases might be related to a general decrease of the emission of precursors of the newly formed particles such as SO_2. However, increasing trends in N/PNC were observed for both UB and TR sites, with a 96 % higher slope in the UB sites. The higher increase of the percentage at the UB sites compared to the TR ones indicates that it probably is the decrease of the condensation sink that increased the Nucleation mode particles, more than the possible abatement effect of DPF of the finest UFP fraction, which was found to be minimal by Damayanti et al. (2023).

It is well accepted that close to roadways an increase in T might yield a decrease in UFP. Thus, Weichenthal et al. (2008) reported that each 10 °C increase in morning temperature was associated with decreases of 14560, 8160 and 11,310 #/cm^3 for UFP exposures in walk, bus, and automobile environments, respectively. On the other side, photochemical nucleation might be influenced by T, RAD and RH conditions (Hamed et al., 2011; Yu et al., 2017; Brines et al., 2015), but also by the CS (Tuovinen et al., 2021, and references therein) which might be reduced at high wind speeds. In urban environments under high insolation Brines et al. (2015) found that nucleation occurred with low CS,

high wind speeds, low RH and high T and insolation. However other global studies found a lower nucleation potential at higher T (Yu et al., 2017). As stated above, the only ss trends were obtained for T (increasing) and RAD (light increase), but not for RH and WS. The results showed that in 4/5 TR sites the Nucleation mode PNC decreased in cities where T increased. Thus, we cannot discard that the dominant decrease of the Nucleation mode particles at the TR sites of this study is influenced, at least partially, by an also generalised T increase. This effect is also possible for the UB sites of DRE, HEL, MUL and ZUR (northern and central Europe), were also a marked Nucleation mode decrease occurs simultaneously with a T increase. On the other hand, in the UB sites of BCN, BUD, LEC, LND, MAD and ROC, the T increase was coincident with an increase of the Nucleation mode, and accordingly an increase of photo-nucleation with T cannot be discarded. Thus, in addition of the effects of the above referred vehicles emission abatement policy actions on Nucleation mode trends, contribution from a generalised urban T increasing trends cannot be discarded. This is also applying to the generalised decreasing trends of the Aitken mode.

The concentrations of the Aitken mode fraction decreased at the majority of sites, most likely due to the previously mentioned reduced emissions of particles from diesel road traffic since EURO 5/V as reported for the street canyon of Marylebone (London) by Damayanti et al. (2023). There was, however, a ss increase at PRA_SUB. These differences are likely to have arisen due to increased road traffic or possibly wood burning.

The trends of the Accumulation mode were similar to that observed for the Aitken mode, most likely due to reduced road traffic solid mode particles due to DPF fitment. However, a non-ss positive trend at PRA_SUB was observed again.

Damayanti et al. (2023) found that for a TR site in London, the concentration of the Aitken mode (30–100 nm in their study), Accumulation mode particles, and BC decreased faster than other pollutants, and declined by −6.2 [−6.5;-5.8], −7.3 [−7.64;-6.99] and −8.3 [−8.56;-7.98]% yr^{-1}, respectively. These slopes were similar to the ones from our study for TR sites (−5.66 [−7.90;-3.42], −6.00 [−7.30;-4.70] and −7.48 [−8.70;-6.26] % yr^{-1}, respectively). They attributed these decreasing trends to the policy interventions in the road transport sector, which effectively decreased emissions of these pollutants. The 2010–2021 decreasing trends found by Damayanti et al. (2023) for the Marylebone (London) TR site are equivalent to a decrease of −242, −643 and −328 # cm^{-3} yr^{-1} for the Nucleation, Aitken and Accumulation modes, respectively. These slopes are all much higher than the ones from our study for TR sites (−144, −380 and −141 # cm^{-3} yr^{-1}, respectively). However, Marylebone Road is a street canyon with >90,000 vehicles day^{-1}, and the effect of the traffic emission controls should be higher than at conventional TR sites. These trends are unlikely to have been substantially influenced by photochemical nucleation, which is observed on only 6 % of days at this site (Bousiotis et al., 2019), and was most notable on the wind sector carrying fresh traffic emissions to the sampler (Damayanti et al., 2023). Also, Chen et al. (2022), for a UB site in northern USA, found 2005–2020 decreases of −26, −99, −63 and −45 # cm^{-3} yr^{-1} for the Nucleation (11–20 nm), Aitken-1 (20–50 nm), Aitken-2 (50–100 nm) and Accumulation (100–500 nm) modes, while the slopes from our study for UB sites were +32 (non-ss), −99(ss) and −58(ss) # cm^{-3} yr^{-1} for the Nucleation, Aitken and Accumulation modes, respectively.

According to the aforementioned study, diesel vehicles in Europe played a predominant role in exhaust PM traffic contributing to ambient PM_{10} and $PM_{2.5}$ concentrations, primarily due to the PM emissions limits for diesel compared to gasoline vehicles. This distinction persisted until the implementation of EURO 5/V and 6/VI standards in 2011 and 2015, respectively, which mandated the use of DPF.

Diesel PM is largely BC, with a major mode at 40–80 nm (Hopke et al., 2022), and a second finer mode of liquid particles from condensed engine oil vapour (Kittelson et al., 2006; Harrison et al., 2018) formed by nucleation of semi-volatile organic compounds (SVOCs) as emissions are diluted and cooled (Charron and Harrison, 2003).

More recently, Giechaskiel et al. (2022) demonstrated that the solid PNC emissions of EURO 6 diesel passenger cars are low due to the implementation of DPF. However, periodically, the trapped particles are oxidised (active regeneration), and the solid PNC emissions during this regeneration are only partly covered by the regulations. Furthermore, the PNC of volatile particles are also not included in the regulations and can be extremely high. Giechaskiel et al. (2022) measured the PNC emissions simultaneously at the tailpipe and the dilution tunnel and found that the weighted (i.e., considering the emissions during regeneration) solid PNC did not exceed the specific limit of 6×10^{11} # km^{-1} for $N_{>23}$. However, the weighted volatile PNC emissions were many orders of magnitude higher, up to 3×10^{13} # km^{-1}. Furthermore, it was found that the volatile PNC were strongly affected by desorption phenomena and that the high volatile PNC during regenerations even interfered with the 10 nm solid PNC measurements at the dilution tunnel, thus having a high impact in the Nucleation mode emissions.

At present, the EU regulates PNC emissions from vehicles only for those >23 nm. Very recently, Lintusaari et al. (2023) showed that the <23 nm particles dominated the non-volatile number concentrations and that the traffic emissions of non-volatile <10 nm particles can be even 3 times higher than those >10 nm. Yet, only a fraction of urban <10 nm particles consisted of non-volatiles.

Accordingly, the emissions of vehicular PM mass decreased markedly since 2011, followed with even larger decreases since 2016 when the implementation of EURO 6/VI required a removal efficiency of 99.9 % of all solid, carbonaceous emissions of UFP (Calderón-Garcidueñas and Ayala, 2022). Furthermore, many of the study cities implemented the Low Emission Zones (LEZ), which have been found to reduce BC concentrations (Holman et al., 2015; Baldauf et al., 2016). However, according to Damayanti et al (2023) the decrease of emissions of Nucleation mode particles during real-world urban driving has been negatively affected by the nucleation of SVOCs that are currently not removed by emission controls. Since the formation of Nucleation mode particles occurs in the diluting exhaust gases, the process is inherently variable, depending upon the dilution ratio and environmental conditions. These factors might account for different trends found for the Nucleation mode in the study cities. Furthermore, the variability of the frequency and intensity of regional (photo) nucleation from precursors emitted from other sources than traffic, such as SO_2 from combustion sources, or of other sources of Nucleation mode particles (industry, shipping or airports) might cause also different trends among cities (Junkermann et al., 2011, 2018; Brines et al., 2015; Salma et al., 2016, 2019; Harrison et al., 2019; Rivas et al., 2020; Trechera et al., 2023).

5. Conclusions

This study evaluates long-term trends (5–11 years in 2009–2019) of ultrafine particle (UFP) concentrations and different particle size modes (UFP ($N_{10\text{-}100}$), PNC ($N_{10\text{-}800}$) and the Nucleation, Aitken and Accumulation modes ($N_{10\text{-}25}$, $N_{25\text{-}100}$ and $N_{100\text{-}800}$, respectively)), based on particle number size distribution (PNSD) data from 21 sites (12 from urban background, 5 from traffic sites, 3 from suburban background and 1 from regional background) from 15 European and 1 US cities. Additionally, the trends in other pollutants and meteorological variables were evaluated in order to support interpretations.

UFP concentrations in urban Europe are largely influenced by road traffic emissions (Trechera et al., 2023, and references therein) as are other pollutants such as NO_X (i.e., NO and NO_2), CO, and BC. Concentrations of SO_2, BC, $PM_{2.5}$ and PM_{10} are influenced by other sources. In most cases European air quality policies resulted in marked reductions of emissions of these pollutants (EEA, 2023).

The results of this study show that in most studied European cities clear abatement of the BC, NO_2, PM, and the Aitken and Accumulation mode particle concentrations followed the implementation of diesel particle filters (DPFs), from 2011 (EURO 5/V), and the subsequent

abatement of NO_X emissions due to the controls required by EURO 6 and VI standards, which came into force in 2015, among other road traffic policies. Other air quality policy measures also generally produced SO_2 and CO decreases.

Reductions in urban NO_X emissions are expected to lead to an increase in O_3 due to a lesser titration by NO and to the reduction of NO_X concentrations in a VOCs-limited O_3 formation regime. This overall behaviour was observed at the majority of sites, especially at the traffic sites. Given the fall in NO_2 and SO_2 concentrations, reduced nitrate and sulphate are also to be expected, and accordingly of PM.

The high influence of the road traffic emissions in the UFP, PNC, BC and NO_2 urban concentrations is also demonstrated by the higher declining slopes reached at the traffic (TR) sites compared to the urban background (UB) ones. Thus, these were 141, 57, 63 and 23 % higher for the Aitken mode particles, Accumulation mode particles, BC and NO_2, respectively.

The trends in the Nucleation mode particles were far more diverse (ss decreases at 6/21 sites and increases at 5/21 sites), with a non-ss increasing trend obtained for the UB sites. However, downward non-ss trends were obtained for the TR and SUB sites. The reduction of the Nucleation mode particles at TR sites was 50, 50, 11 and 93 % lower than those obtained for Aitken and Accumulation mode particles, NO_X and BC, respectively. This is most probably due to inefficient removal of the semi-volatile diesel particle fraction by DPFs and a contribution from gasoline vehicles, expected to be predominantly in this size range, as previously reported by Chen et al. (2022) and Damayanti et al. (2023) for specific sites from US and Europe. These varying trends in the Nucleation mode particle number concentration are also affecting the UFP and total PNC trends, because of the high proportion of the Nucleation mode particles in both concentration ranges. Also the 9-fold decrease of BC versus NO_X is probably result of the efficient impact of EURO 5 DPFs in abating ambient BC and the negative effect of the 'diesel gate' on ambient NO_X.

The diverse trends obtained for the Nucleation mode particles in UB sites might be due not only to the lack of emission controls for semi-volatile organic compounds escaping from DPFs, but also due to a reduction in condensation sink potential, which facilitates new particle formation. Moreover, at some sites, the presence of other substantial lower-mode UFP sources, such as photochemical nucleation, industry, shipping and aircraft emissions, also influence the trend of the Nucleation mode.

Moreover, the urban T increasing trends might have also influenced those of PNC, Nucleation and Aitken modes. The results showed that for some sites the decrease of the Nucleation mode particles might be influenced by a T increase, but also that in other sites an increase of photo-nucleation might be associated to a T increase.

Overall, the results presented here demonstrate the positive effects of the air quality policies implemented in Europe in abating air pollutants, including the Aitken and Accumulation mode particles, but less for the Nucleation mode. The different modes of the PNSD should be evaluated independently to assess further policies promulgated to abate urban UFPs.

CRediT authorship contribution statement

Meritxell Garcia-Marlès: Conceptualization, Data curation, Formal analysis, Methodology, Writing – original draft, Writing – review & editing. **Rosa Lara:** Conceptualization, Data curation, Formal analysis, Methodology, Writing – original draft, Writing – review & editing. **Cristina Reche:** Data curation, Writing – review & editing. **Noemí Pérez:** Data curation, Writing – review & editing. **Aurelio Tobías:** Methodology, Writing – review & editing. **Marjan Savadkoohi:** Data curation, Writing – review & editing. **David Beddows:** Data curation, Writing – review & editing. **Imre Salma:** Data curation, Writing – review & editing. **Máté Vörösmarty:** Data curation, Writing – review & editing. **Tamás Weidinger:** Data curation, Writing – review & editing. **Christoph Hueglin:** Data curation, Writing – review & editing. **Nikos Mihalopoulos:** Data curation, Writing – review & editing. **Georgios Grivas:** Data curation, Writing – review & editing. **Panayiotis Kalkavouras:** Data curation, Writing – review & editing. **Jakub Ondráček:** Data curation, Writing – review & editing. **Naděžda Zíková:** Data curation, Writing – review & editing. **Jarkko V. Niemi:** Data curation, Writing – review & editing. **Hanna E. Manninen:** Data curation, Writing – review & editing. **David C. Green:** Data curation, Writing – review & editing. **Anja H. Tremper:** Data curation, Writing – review & editing. **Michael Norman:** Data curation, Writing – review & editing. **Stergios Vratolis:** Data curation, Writing – review & editing. **Konstantinos Eleftheriadis:** Data curation, Writing – review & editing. **Francisco J. Gómez-Moreno:** Data curation, Writing – review & editing. **Elisabeth Alonso-Blanco:** Data curation, Writing – review & editing. **Alfred Wiedensohler:** Data curation, Writing – review & editing. **Kay Weinhold:** Data curation, Writing – review & editing. **Maik Merkel:** Data curation, Writing – review & editing. **Susanne Bastian:** Data curation, Writing – review & editing. **Barbara Hoffmann:** Data curation, Writing – review & editing. **Hicran Altug:** Data curation, Writing – review & editing. **Jean-Eudes Petit:** Data curation, Writing – review & editing. **Olivier Favez:** Data curation, Writing – review & editing. **Sebastiao Martins Dos Santos:** Data curation, Writing – review & editing. **Jean-Philippe Putaud:** Data curation, Writing – review & editing. **Adelaide Dinoi:** Data curation, Writing – review & editing. **Daniele Contini:** Data curation, Writing – review & editing. **Hilkka Timonen:** Data curation, Writing – review & editing. **Janne Lampilahti:** Data curation, Writing – review & editing. **Tuukka Petäjä:** Data curation, Writing – review & editing. **Marco Pandolfi:** Data curation, Writing – review & editing. **Philip K. Hopke:** Conceptualization, Data curation, Writing – review & editing. **Roy M. Harrison:** Conceptualization, Data curation, Writing – review & editing. **Andrés Alastuey:** Conceptualization, Data curation, Writing – original draft, Writing – review & editing. **Xavier Querol:** Conceptualization, Data curation, Methodology, Supervision, Writing – original draft, Writing – review & editing.

Declaration of competing interest

The authors declare that they have no known competing financial interests or personal relationships that could have appeared to influence the work reported in this paper.

Data availability

Data will be made available on request.

Acknowledgements

This study is supported by the RI-URBANS project (Research Infrastructures Services Reinforcing Air Quality Monitoring Capacities in European Urban & Industrial Areas, European Union's Horizon 2020 research and innovation program, Green Deal, European Commission, contract 101036245), the "Agencia Estatal de Investigación" from the Spanish Ministry of Science and Innovation, FEDER funds under the projects AIRPHONEMA (PID2022-142160OB-I00), and the Generalitat de Catalunya (AGAUR 2021 SGR 00447). This research is partly supported by the Hungarian Research, Development and Innovation Office (grant no. K132254).

We would like to thank also to ACTRIS for providing PNC-PNSD datasets for a number of sites of this study, and National and City authorities for providing others.

Appendix A. Supplementary material

Supplementary data to this article can be found online at https://doi.org/10.1016/j.envint.2024.108510.

References

Aas, W., Mortier, A., Bowersox, V., Cherian, R., Faluvegi, G., Fagerli, H., Hand, J., Klimont, Z., Galy-Lacaux, C., Lehmann, C.M.B., Myhre, C.L., Myhre, G., Olivié, D., Sato, K., Quaas, J., Rao, P.S.P., Schulz, M., Shindell, D., Skeie, R.B., Stein, A., Takemura, T., Tsyro, S., Vet, R., Xu, X., 2019. Global and regional trends of atmospheric sulfur. Sci. Rep. 9 (1), 953. https://doi.org/10.1038/s41598-018-37304-0.

ACTRIS, C. for A.I.-S.M., Preliminary, 2021. Preliminary ACTRIS recommendation for aerosol in-situ sampling, measurements, and analysis. https://www.actris.eu/sites/default/files/2021-06/Preliminary%20ACTRIS%20recommendations%20for%20aerosol%20in-situ%20measurements%20June%202021.pdf.

Amato, F., Alastuey, A., Karanasiou, A., Lucarelli, F., Nava, S., Calzolai, G., Severi, M., Becagli, S., Gianelle, V.L., Colombi, C., Alves, C., Custódio, D., Nunes, T., Cerqueira, M., Pio, C., Eleftheriadis, K., Diapouli, E., Reche, C., Minguillón, M.C., Manousakas, M.-I., Maggos, T., Vratolis, S., Harrison, R.M., Querol, X., 2016. AIRUSE-LIFE+: a harmonized PM speciation and source apportionment in five southern European cities. Atmos. Chem. Phys. 16, 3289–3309. https://doi.org/10.5194/acp-16-3289-2016.

Anenberg, S., Miller, J., Minjares, R., Du, L., Henze, D.K., Lacey, F., Malley, C.S., Emberson, L.S., Franco, V., Klimont, Z., Heyes, C.h., 2017. Impacts and mitigation of excess diesel-related NOx emissions in 11 major vehicle markets. Nature 545, 467–471. https://doi.org/10.1038/nature22086.

Baldauf, R.W., Devlin, R.B., Gehr, P., Giannelli, R., Hassett-Sipple, B., Jung, H., Martini, G., McDonald, J., Sacks, J.D., Walker, K., 2016. Ultrafine particle metrics and research considerations: review of the 2015 UFP workshop. Int. J. Environ. Res. Public Health 13, 1054. https://doi.org/10.3390/ijerph13111054.

Balduzzi, S., Rücker, G., Schwarzer, G., 2019. How to perform a meta-analysis with R: a practical tutorial. Evid. Based Ment. Health 22, 153–160. https://doi.org/10.1136/ebmental-2019-300117.

Beddows, D.C.S., Harrison, R.M., Green, D.C., Fuller, G.W., 2015. Receptor modelling of both particle composition and size distribution from a background site in London. UK. Atmos. Chem. Phys. 15, 10107–10125. https://doi.org/10.5194/acp-15-10107-2015.

Beddows, D.C.S., Harrison, R.M., 2019. Receptor modelling of both particle composition and size distribution from a background site in London, UK – a two-step approach. Atmos. Chem. Phys. 19, 4863–4876. https://doi.org/10.5194/acp-19-4863-2019.

Benavides, J., Guevara, M., Snyder, M.G., Rodríguez-Rey, D., Soret, A., Pérez García-Pando, C., Jorba, O., 2021. On the impact of excess diesel NOx emissions upon NO_2 pollution in a compact city. Environ. Res. Lett. 16 (2), 024024 https://doi.org/10.1088/1748-9326/abd5dd.

Bousiotis, D., Dall'Osto, M., Beddows, D.C.S., Pope, F.D., Harrison, R.M., 2019. Analysis of new particle formation (NPF) events at nearby rural, urban background and urban roadside sites. Atmos. Chem. Phys. 19, 5679–5694. https://doi.org/10.5194/acp-19-5679-2019.

Brines, M., Dall'Osto, M., Beddows, D.C.S., Harrison, R.M., Querol, X., 2014. Simplifying aerosol size distribution modes simultaneously detected at four monitoring sites during SAPUSS. Atmos. Chem. Phys. 14, 2973–2986. https://doi.org/10.5194/acp-14-2973-2014.

Brines, M., Dall'Osto, M., Beddows, D.C.S., Harrison, R.M., Gómez-Moreno, F., Núñez, L., Artíñano, B., Costabile, F., Gobbi, G.P., Salimi, F., Morawska, L., Sioutas, C., Querol, X., 2015. Traffic and nucleation events as main sources of ultrafine particles in high-insolation developed world cities. Atmos. Chem. Phys. 15, 5929–5945. https://doi.org/10.5194/acp-15-5929-2015.

Calderón-Garcidueñas, L., Ayala, A., 2022. Air pollution, ultrafine particles, and your brain: are combustion nanoparticle emissions and engineered nanoparticles causing preventable fatal neurodegenerative diseases and common neuropsychiatric outcomes? Environ. Sci. Technol. 56 (11), 6847–6856. https://doi.org/10.1021/acs.est.1c04706.

Carslaw, D.C., Ropkins, K., 2012. Openair - an R package for air quality data analysis. Environ. Model. Software 27 (28), 52–61. https://doi.org/10.1016/j.envsoft.2011.09.008.

Carslaw, D.C., Murrells, T.P., Andersson, J., Keenan, M., 2016. Have vehicle emissions of primary NO_2 peaked? Faraday Discuss. 189, 439–454. https://doi.org/10.1039/c5fd00162e.

Cassee, F., Morawska, L., Peters, A., 2019. The White Paper on Ambient Ultrafine Particles: evidence for policy makers. 'Thinking outside the box' Team, 23 pp, https://efca.net/files/WHITE%20PAPER-UFP%20evidence%20for%20policy%20makers%20(25%20OCT).pdf.

CEN, 2020. CEN/TS 17434:2020. CEN Standard for Ambient air - Determination of the particle number size distribution of atmospheric aerosol using a Mobility Particle Size Spectrometer (MPSS). https://standards.iteh.ai/catalog/standards/cen/a841bc08-ed34-4fa8-94ca-8c5e07b99db9/cen-ts-17434-2020.

Charron, A., Harrison, R.M., 2003. Primary particle formation from vehicle emissions during exhaust dilution in the roadside atmosphere. Atmos. Environ. 37 (29), 4109–4119. https://doi.org/10.1016/S1352-2310(03)00510-7.

Chen, Y., Masiol, M., Squizzato, S., Chalupa, D.C., Zíková, N., Pokorná, P., Rich, D.Q., Hopke, P.K., 2022. Long-term trends of ultrafine and fine particle number concentrations in New York State: apportioning between emissions and dispersion. Environ. Pollut. 310, 119797 https://doi.org/10.1016/j.envpol.2022.119797.

Chen, D.G.D., Peace, K.E., 2013. Applied Meta-Analysis with R. CRC Press.

Cleveland, R.B., Cleveland, W.S., McRae, J.E., Terpenning, I., 1990. STL: A seasonal-trend decomposition. J. off. Stat 6 (1), 3–73.

Colette, A., Granier, C., Hodnebrog, Ø., Jakobs, H., Maurizi, A., Nyiri, A., Bessagnet, B., D'Angiola, A., D'Isidoro, M., Gauss, M., Meleux, F., Memmesheimer, M., Mieville, A., Rouïl, L., Russo, F., Solberg, S., Stordal, F., Tampieri, F., 2011. Air quality trends in Europe over the past decade: a first multi-model assessment. Atmos. Chem. Phys. 11, 11657–11678. https://doi.org/10.5194/acp-11-11657-2011.

Crippa, M., Janssens-Maenhout, G., Dentener, F., Guizzardi, D., Sindelarova, K., Muntean, M., Van Dingenen, R., Granier, C., 2016. Forty years of improvements in European air quality: regional policy-industry interactions with global impacts. Atmos. Chem. Phys. 16, 3825–3841. https://doi.org/10.5194/acp-16-3825-2016.

Dahl, A., Gharibi, A., Swietlicki, E., Gudmundsson, A., Bohgard, M., Ljungman, A., Blomqvist, G., Gustafsson, M., 2006. Traffic-generated emissions of ultrafine particles from pavement-tire interface. Atmos. Environ. 40 (7), 1314–1323. https://doi.org/10.1016/j.atmosenv.2005.10.029.

Dall'Osto, M., Thorpe, A., Beddows, D.C.S., Harrison, R.M., Barlow, J.F., Dunbar, T., Williams, P.I., Coe, H., 2011. Remarkable dynamics of nanoparticles in the urban atmosphere. Atmos. Chem. Phys. 11, 6623–6637. https://doi.org/10.5194/acp-11-6623-2011.

Damayanti, S., Harrison, R.M., Pope, F., Beddows, D.C.S., 2023. Limited impact of diesel particle filters on road traffic emissions of ultrafine particles. Environ. Int. 174, 107888 https://doi.org/10.1016/j.envint.2023.107888.

Port de Barcelona, 2023. Estadísticas del Puerto de Barcelona. https://www.portdebarcelona.cat/es/web/autoritat-portuaria/estadisticas.

Degraeuwe, B., Thunis, P., Clappier, A., Weiss, M., Lefebvre, W., Janssen, S., Vranckx, S., 2017. Impact of passenger car NOX emissions on urban NO2 pollution – scenario analysis for 8 European cities. Atmos. Environ. 171, 330–337. https://doi.org/10.1016/j.atmosenv.2017.10.040.

Dinoi, A., Gulli, D., Ammoscato, I., Calidonna, C.R., Contini, D., 2021. Impact of the coronavirus pandemic lockdown on atmospheric nanoparticle concentrations in two sites of Southern Italy. Atmos. 12, 352. https://doi.org/10.3390/atmos12030352.

Eleftheriadis, K., Gini, M.I., Diapouli, E., Vratolis, S., Vasilatou, V., Fetfatzis, P., Manousakas, M.I., 2021. Aerosol microphysics and chemistry reveal the COVID19 lockdown impact on urban air quality. Sci. Rep. 11, 14477. https://doi.org/10.1038/s41598-021-93650-6.

EMEP, 2016. EMEP Co-operative Programme for Monitoring and Evaluation of the Long-range Transmission of Air Pollutants in Europe: Air pollution trends in the EMEP region between 1990 and 2012. EMEP/CCC-Report 1/2016, 105 pp. https://projects.nilu.no/ccc/reports/cccr1-2016.pdf.

US EPA, 2019. Integrated Science Assessment (ISA) for Particulate Matter (Final Report, Dec 2019). U.S. Environmental Protection Agency, Washington, DC, EPA/600/R-19/188. https://www.federalregister.gov/documents/2020/01/27/2020-01223/integrated-science-assessment-for-particulate-matter.

ETC, 2020. Understanding Air Quality Trends in Europe. Eionet Report - ETC/ATNI 2020/8, 38 pp. ISBN 978-82-93752-15-8.

Escudero, M., Lozano, A., Hierro, J., del Valle, J., Mantilla, E., 2014. Urban influence on increasing ozone concentrations in a characteristic Mediterranean agglomeration. Atmos. Environ. 99, 322–332. https://doi.org/10.1016/j.atmosenv.2014.09.061.

Genc, S., Zadeoglulari, Z., Fuss, S.H., Genc, K., 2012. The adverse effects of air pollution on the nervous system. J. Toxicol., 782462 https://doi.org/10.1155/2012/782462.

Giechaskiel, B., Melas, A., Lähde, T., 2022. Detailed characterization of solid and volatile particle emissions of two euro 6 diesel vehicles. Appl. Sci. 12 (7), 3321. https://doi.org/10.3390/app12073321.

Grange, S.K., Farren, N.J., Vaughan, A.R., Davison, J., Carslaw, D.C., 2020. Post-dieselgate: evidence of NOx emission reductions using on-road remote sensing. Environ. Sci. Technol. Lett. 7 (6), 382–387. https://doi.org/10.1021/acs.estlett.0c00188.

Hamed, A., Korhonen, H., Sihto, S.L., Joutsensaari, J., Järvinen, H., Petäjä, T., Arnold, F., Nieminen, T., Kulmala, M., Smith, J.N., Lehtinen, K.E.J., Laaksonen, A., 2011. The role of relative humidity in continental new particle formation. J. Geophys. Res. 116, D03202. https://doi.org/10.1029/2010JD014186.

Harrison, R.M., Beddows, D.C.S., Dall'Osto, M.,, 2011. PMF analysis of wide-range particle size spectra collected on a major highway. Environ. Sci. Technol. 45, 5522–5528. https://doi.org/10.1021/es2006622.

Harrison, R.M., Rob MacKenzie, A., Xu, H., Alam, M.S., Nikolova, I., Zhong, J., Singh, A., Zeraati-Rezaei, S., Stark, C., Beddows, D.C.S., Liang, Z., Xu, R., Cai, X., 2018. Diesel exhaust nanoparticles and their behaviour in the atmosphere. Proc. Math. Phys. Eng. Sci. 474 (2220), 20180492. https://doi.org/10.1098/rspa.2018.0492.

Harrison, R.M., Beddows, D.C.S., Alam, M.S., Singh, A., Brean, J., Xu, R., Kotthaus, S., Grimmond, S., 2019. Interpretation of particle number size distributions measured across an urban area during the FASTER campaign. Atmos. Chem. Phys. 19, 39–55. https://doi.org/10.5194/acp-19-39-2019.

Holman, C., Harrison, R.M., Querol, X., 2015. Review of the efficacy of low emission zones to improve urban air quality in European cities. Atmos. Environ. 111, 161–169. https://doi.org/10.1016/j.atmosenv.2015.04.009.

Hopke, P.K., Feng, Y., Dai, Q., 2022. Source apportionment of particle number concentrations: a global review. Sci. Total Environ. 819, 153104 https://doi.org/10.1016/j.scitotenv.2022.153104.

Ibald-Mulli, A., Wichmann, H.E., Kreyling, W., Peters, A., 2004. Epidemiological evidence on health effects of ultrafine particles. J. Aerosol Med. 15 (2), 189–201. https://doi.org/10.1089/089426802320282310.

ICCT, 2016. A technical summary of EURO 6/VI vehicle emission standards – International Council on Clean Transportation, 12p. https://theicct.org/publication/a-technical-summary-of-euro-6-vi-vehicle-emission-standards/.

ISO, 2023. ISO 80004-1:2023. Nanotechnologies – Vocabulary — Part 1: Core vocabulary. https://www.iso.org/standard/79525.html.

Junkermann, W., Hacker, J., 2018. Ultrafine particles in the lower troposphere: major sources, invisible plumes, and meteorological transport processes. Bull. Am. Meteorol. Soc. 99, 2587–2602. https://doi.org/10.1175/BAMS-D-18-0075.1.

Junkermann, W., Hagemann, R., Vogel, B., 2011. Nucleation in the Karlsruhe plume during the COPS/TRACKS-Lagrange experiment. Quart. J. Royal Meteorol. Soc. 137, 267–274. https://doi.org/10.1002/qj.753.

Kittelson, D.B., Watts, W.F., Johnson, J.P., 2006. On-road and laboratory evaluation of combustion aerosols – Part 1: Summary of diesel engine results. J. Aerosol Sci. 37 (8), 913–930. https://doi.org/10.1016/j.jaerosci.2005.08.005.

Kreyling, W.G., Hirn, S., Möller, W., Schleh, C., Wenk, A., Celik, G., Lipka, J., Schäffler, M., Haberl, N., Johnston, B.D., Sperling, R., Schmid, G., Simon, U., Parak, W.J., Semmler-Behnke, M., 2014. Air-blood barrier translocation of tracheally instilled gold nanoparticles inversely depends on particle size. ACS Nano 8 (1), 222–233. https://doi.org/10.1021/nn403256v.

Kuenen, J., Visschedijk, A., Heslinga, D., 2022. Dataset on PM ultrafine and non-exhaust sectoral emission distribution over Europe and pilot cities. RI-URBANS report M13, 7 pp, https://riurbans.eu/wp-content/uploads/2022/11/RI-URBANS_M13_.pdf.

Kulmala, M., Kerminen, V.M., Petaja, T., Ding, A.J., Wang, L., 2017. Atmospheric gas-to-particle conversion: why NPF events are observed in megacities? Faraday Discuss. 200, 271–288. https://doi.org/10.1039/c6fd00257a.

Li, Q.Q., Guo, Y.T., Yang, J.Y., Liang, C.S., 2023. Review on main sources and impacts of urban ultrafine particles: traffic emissions, nucleation, and climate modulation. Atmosph. Environ. 19, 100221 https://doi.org/10.1016/j.aeaoa.2023.100221.

Lintusaari, H., Kuuluvainen, H., Vanhanen, J., Salo, L., Portin, H., Järvinen, A., Juuti, P., Hietikko, R., Teinilä, K., Timonen, H., Niemi, J.V., Rönkkö, T., 2023. Sub-23 nm particles dominate non-volatile particle number emissions of road traffic. Environ. Sci. Technol. 57 (29), 10763–10772. https://doi.org/10.1021/acs.est.3c03221.

Mathissen, M., Scheer, V., Vogt, R., Benter, T., 2011. Investigation on the potential generation of ultrafine particles from the tire-road interface. Atmosph. Environ. 45 (34), 6172–6179. https://doi.org/10.1016/j.atmosenv.2011.08.032.

McMurry, P.H., Friedlander, S.K., 1979. New particle formation in the presence of an aerosol. Atmos. Environ. 13, 1635–1651. https://doi.org/10.1016/0004-6981(79)90322-6.

Mikkonen, S., Németh, Z., Varga, V., Weidinger, T., Leinonen, Y.-J., T., Salma, I.,, 2020. Decennial time trends and diurnal patterns of particle number concentrations in a Central European city between 2008 and 2018. Atmos. Chem. Phys. 20, 12247–12263. https://doi.org/10.5194/acp-20-12247-2020.

Monks, P.S., Archibald, A.T., Colette, A., Cooper, O., Coyle, M., Derwent, R., Fowler, D., Granier, C., Law, K.S., Mills, G.E., Stevenson, D.S., Tarasova, O., Thouret, V., von Schneidemesser, E., Sommariva, R., Wild, O., Williams, M.L., 2015. Tropospheric ozone and its precursors from the urban to the global scale from air quality to short-lived climate forcer. Atmos. Chem. Phys. 15, 8889–8973. https://doi.org/10.5194/acp-15-8889-2015.

Niemann, H., Winner, H., Asbach, C., Kaminski, H., Frentz, G., Milczarek, R., 2020. Influence of disc temperature on ultrafine, fine, and coarse particle emissions of passenger car disc brakes with organic and inorganic pad binder materials. Atmos. 11 (10), 1060. https://doi.org/10.3390/atmos11101060.

Oberdörster, G., Sarp, Z., Atudorei, V., Elder, A., Gelein, R., Kreyling, W., Cox, C., 2004. Translocation of Inhaled Ultrafine Particles to the Brain. Inhal. Toxicol. 16 (6–7), 437–445. https://doi.org/10.1080/08958370490439597.

Oberdörster, G., Oberdörster, E., Oberdörster, J., 2005. Nanotoxicology: an emerging discipline evolving from studies of ultrafine particles. Environ. Health Perspect. 113, 823–839. https://doi.org/10.1289/ehp.7339.

Ohlwein, S., Kappeler, R., Kutlar Joss, M., Künzli, N., Hoffmann, B., 2019. Health effects of ultrafine particles: a systematic literature review update of epidemiological evidence. Int. J. Public Health 64 (4), 547–559. https://doi.org/10.1007/s00038-019-01202-7.

Peters, A., Veronesi, B., Calderón-Garcidueñas, L., Gehr, P., Chen, L.C., Geiser, M., Reed, W., Rothen-Rutishauser, B., Schürch, S., Schulz, H., 2006. Translocation and potential neurological effects of fine and ultrafine particles a critical update. Part. Fibre. Toxicol. 3, 13. https://doi.org/10.1186/1743-8977-3-13.

Petit, J.E., Dupont, J.C., Favez, O., Gros, V., Zhang, Y., Sciare, J., Simon, L., Truong, F., Bonnaire, N., Amodeo, T., Vautard, R., Haeffelin, M., 2021. Response of atmospheric composition to COVID-19 lockdown measures during spring in the Paris region (France). Atmos. Chem. Phys. 21 (22), 17167–17183. https://doi.org/10.5194/acp-21-17167-2021.

Pey, J., Querol, X., Alastuey, A., Rodríguez, S., Putaud, J.P., Van Dingenen, R., 2009. Source Apportionment of urban fine and ultrafine particle number concentration in a Western Mediterranean city. Atmos. Environ. 43, 4407–4415. https://doi.org/10.1016/j.atmosenv.2009.05.024.

Presto, A.A., Saha, P.K., Robinson, A.L., 2021. Past, present, and future of ultrafine particle exposures in North America. Atmosph. Environ. 10, 100109 https://doi.org/10.1016/j.aeaoa.2021.100109.

Putaud, J.P., Pisoni, E., Mangold, A., Hueglin, C., Sciare, J., Pikridas, M., Savvides, C., Ondracek, J., Mbengue, S., Wiedensohler, A., Weinhold, K., Merkel, M., Poulain, L., van Pinxteren, D., Herrmann, H., Massling, A., Nordstroem, C., Alastuey, A., Reche, C., Pérez, N., Castillo, S., Sorribas, M., Adame, J.A., Petaja, T., Lehtipalo, K., Niemi, J., Riffault, V., de Brito, J.F., Colette, A., Favez, O., Petit, J.E., Gros, V., Gini, M.I., Vratolis, S., Eleftheriadis, K., Diapouli, E., Denier van der Gon, H., Yttri, K. E., Aas, W., 2023. Impact of 2020 COVID-19 lockdowns on particulate air pollution across Europe. Atmos. Chem. Phys. 23, 10145–10161. https://doi.org/10.5194/acp-23-10145-2023.

Putaud, J.P., Pozzoli, L., Pisoni, E., Martins Dos Santos, S., Lagler, F., Lanzani, G., Dal Santo, U., Colette, A., 2021. Impacts of the COVID-19 lockdown on air pollution at regional and urban background sites in northern Italy. Atmos. Chem. Phys. 21, 7597–7609. https://doi.org/10.5194/acp-21-7597-2021.

R Core Team, 2023. R: A Language and Environment for Statistical Computing. R Foundation for Statistical Computing, Vienna, Austria https://www.R-project.org/.

RI-URBANS, 2022. Guidelines, datasets of non-regulated pollutants incl. metadata, methods. Deliverable D1 (D1.1). 71 pp. https://riurbans.eu/wp-content/uploads/2022/10/RI-URBANS_D1_D1_1.pdf.

Rivas, I., Beddows, D.C.S., Amato, F., Green, D.C., Järvi, L., Hueglin, C., Reche, C., Timonen, H., Fuller, G.W., Niemi, J.V., Pérez, N., Aurela, M., Hopke, P.K., Alastuey, A., Kulmala, M., Harrison, R.M., Querol, X., Kelly, F.J., 2020. Source apportionment of particle number size distribution in urban background and traffic stations in four European cities. Environ. Int. 135, 105345 https://doi.org/10.1016/j.envint.2019.105345.

Salma, I., Németh, Z., 2019. Dynamic and timing properties of new aerosol particle formation and consecutive growth events. Atmos. Chem. Phys. 19, 5835–5852. https://doi.org/10.5194/acp-19-5835-2019.

Salma, I., Németh, Z., Kerminen, V.-M., Aalto, P., Nieminen, T., Weidinger, T., Molnár, Á., Imre, K., Kulmala, M., 2016. Regional effect on urban atmospheric nucleation. Atmos. Chem. Phys. 16, 8715–8728. https://doi.org/10.5194/acp-16-8715-2016.

Salma, I., Vörösmarty, M., Gyöngyösi, A.Z., Thén, W., Weidinger, T., 2020. What can we learn about urban air quality with regard to the first outbreak of the COVID-19 pandemic? A case study from central Europe. Atmos. Chem. Phys. 20, 15725–15742. https://doi.org/10.5194/acp-20-15725-2020.

Savadkoohi, M., Pandolfi, M., Reche, C., Niemi, J.V., Mooibroek, D., Titos, G., Green, D. C., Tremper, A.H., Hueglin, C., Liakakou, E., Mihalopoulos, N., Stavroulau, I., Artiñano, B., Coz, E., Alados-Arboledas, L., Beddows, D., Riffault, V., De Brito, J.F., Bastian, S., Baudic, A., Colombi, C., Constabile, F., Chazeau, B., Marchand, N., Gómez-Amo, J.L., Estellés, V., Matos, V., van der Gaag, E., Gille, G., Luoma, K., Manninen, H.E., Norman, M., Silvergren, S., Petit, J.-E., Putaud, J.-P., Rattigan, O.V., Timonen, H., Tuch, T., Merkel, M., Weinhold, K., Vratolis, S., Vasilescu, J., Favez, O., Harrison, R.M., Laj, P., Wiedensohler, A., Hopke, P.K., Petäjä, T., Alastuey, A., Querol, X., 2023. The variability of mass concentrations and source apportionment analysis of equivalent black carbon across urban Europe. Environ. Int. 178, 108081 https://doi.org/10.1016/j.envint.2023.108081.

Schwarz, M., Schneider, A., Cyrys, J., Bastian, S., Breitner, S., Peters, A., 2023. Impact of ambient ultrafine particles on cause-specific mortality in three german cities. Am. J. Respir. Crit. Care Med. 207 (10), 1334–1344. https://doi.org/10.1164/rccm.202209-1837OC.

Seinfeld, J.H., Pandis, S., 2016. Atmospheric Chemistry and Physics: From Air Pollution to Climate Change. third ed., Wiley. ISBN 10: 1118947401.

Sen, P.K., 1968. Estimates of the regression coefficient based on Kendall's Tau. J. Am. Stat. Assoc. 63, 1379–1389.

Sicard, P., Agathokleous, E., De Marco, A., Paoletti, E., Calatayud, V., 2021. Urban population exposure to air pollution in Europe over the last decades. Environ. Sci. Eur. 33, 28. https://doi.org/10.1186/s12302-020-00450-2.

Simon, M.C., Naumova, E.N., Levy, J.I., Brugge, D., Durant, J.L., 2020. Ultrafine particle number concentration model for estimating retrospective and prospective long-term ambient exposures in urban neighborhoods. Environ. Sci. Technol. 54 (3), 1677–1686. https://doi.org/10.1021/acs.est.9b03369.

Spracklen, D.V., Carslaw, K.S., Merikanto, J., Mann, G.W., Reddington, C.L., Pickering, S., Ogren, J.A., Andrews, E., Baltensperger, U., Weingartner, E., Boy, M., Kulmala, M., Laakso, L., Lihavainen, H., Kivekäs, N., Komppula, M., Mihalopoulos, N., Kouvarakis, G., Jennings, S.G., O'Dowd, C., Birmili, W., Wiedensohler, A., Weller, R., Gras, J., Laj, P., Sellegri, K., Bonn, B., Krejci, R., Laaksonen, A., Hamed, A., Minikin, A., Harrison, R.M., Talbot, R., Sun, J., 2010. Explaining global surface aerosol number concentrations in terms of primary emissions and particle formation. Atmos. Chem. Phys. 10, 4775–4793. https://doi.org/10.5194/acp-10-4775-2010.

Stacey, B., Harrison, R.M., Pope, F., 2020. Evaluation of ultrafine particle concentrations and size distributions at London Heathrow Airport. Atmosph. Environ. 222, 117148 https://doi.org/10.1016/j.atmosenv.2019.117148.

Theil, H., 1992. A rank-invariant method of linear and polynomial regression analysis. In: Raj, B., Koerts, J. (Eds.), Henri Theil's Contributions to Economics and Econometrics, Advanced Studies in Theoretical and Applied Econometrics, vol. 23. Springer, Dordrecht. https://doi.org/10.1007/978-94-011-2546-8_20.

Tobías, A., Rivas, I., Reche, C., Alastuey, A., Rodríguez, S., Fernández-Camacho, R., Sánchez de la Campa, A.M., de la Rosa, J., Sunyer, J., Querol, X., 2018. Short-term effects of ultrafine particles on daily mortality by primary vehicle exhaust versus secondary origin in three Spanish cities. Environ. Int. 111, 144–151. https://doi.org/10.1016/j.envint.2017.11.015.

Trechera, P., Garcia-Marlès, M., Liu, X.S., Reche, C., Perez, N., Savadkoohi, M., Beddows, D., Salma, I., Vörösmarty, M., Casans, A., Casquero-Vera, J.A., Hueglin, C., Marchand, N., Chazeau, B., Gille, G., Kalkavouras, P., Mihalopoulos, N., Ondracek, J., Zíková, N., Niemi, J.V., Manninen, H.E., Green, D.C., Tremper, A.H., Norman, M., Vratolis, S., Eleftheriadis, K., Gomez-Moreno, F.J., Alonso-Blanco, E., Gerwig, H., Wiedensohler, A., Weinhold, K., Merkel, M., Bastian, S., Petit, J.E., Favez, O., Crumeyrolle, S., Ferlay, N., Dos Santos, S.M., Putaud, J.P., Timonen, H., Lampilahti, J., Asbach, C., Wolf, C., Kaminski, H., Altug, H., Hoffmann, B., Rich, D. Q., Pandolfi, M., Harrison, R.M., Hopke, P.K., Petaja, T., Alastuey, A., Querol, X., 2023. Phenomenology of ultrafine particle concentrations and size distribution across urban Europe. Environ. Int. 172, 107744 https://doi.org/10.1016/j.envint.2023.107744.

Tuovinen, S., Kontkanen, J., Cai, R., Kulmala, M., 2021. Condensation sink of atmospheric vapors: the effect of vapor properties and the resulting uncertainties. Environ. Sci. Atmos. 1, 543–557. https://doi.org/10.1039/D1EA00032B.

Weichenthal, S., Dufresne, A., Infante-Rivard, C., Joseph, L., 2008. Determinants of ultrafine particle exposures in transportation environments: findings of an 8-month survey conducted in Montréal, Canada. J. Expo. Sci. Environ. Epidemiol. 18, 551–563. https://doi.org/10.1038/sj.jes.7500644.

WHO, 2021a. Ambient (outdoor) air pollution. World Health Organization. https://www.who.int/news-room/fact-sheets/detail/ambient-(outdoor)-air-quality-and-health.

WHO, 2021b. WHO global air quality guidelines: particulate matter (PM2.5 and PM10), ozone, nitrogen dioxide, sulfur dioxide and carbon monoxide. World Health Organization. 273 pp, https://apps.who.int/iris/handle/10665/345329.

Wichmann, H.E., Spix, C., Tuch, T., Wölke, G., Peters, A., Heinrich, J., Kreyling, W.G., Heyder, J., 2000. Daily mortality and fine and ultrafine particles in Erfurt, Germany part I: role of particle number and particle mass. Rep. Health Effects Inst. 98, 5–98. PMID: 11918089.

Yu, F., Luo, G., Nadykto, A.B., Herb, J., 2017. Impact of temperature dependence on the possible contribution of organics to new particle formation in the atmosphere. Atmos. Chem. Phys. 17, 4997–5005. https://doi.org/10.5194/acp-17-4997-2017.

Yu, X., Venecek, M., Kumar, A., Hu, J., Tanrikulu, S., Soon, S.T., Tran, C., Fairley, D., Kleeman, M.J., 2019. Regional sources of airborne ultrafine particle number and mass concentrations in California. Atmos. Chem. Phys. 19 (23), 14677–14702. https://doi.org/10.5194/acp-19-14677-2019.

Zhou, L., Hopke, P.K., Stanier, C.O., Pandis, S.N., Ondov, J.M., Pancras, J.P., 2005. Investigation of the relationship between chemical composition and size distribution of airborne particles by partial least squares and positive matrix factorization. J. Geophys. Res. 110, D07S18. https://doi.org/10.1029/2004JD005050.